Table 2
Differential gene expression patterns in αGC-treated and OCH-treated murine NKT cells

		Liver CD3+NK1.1+							Spleen CD3+NK1.1+						
		Untreated	αGC		OCH				Untreated	αGC		OCH			
Common name	GenBank		1.5 h		12 h		1.5 h		12 h		1.5 h		12 h		1.5 h		12 h	
IFN-γ	K00083	1.0 P	5.0	P	0.3	P	1.2	P	0.1	P	1.0 P	4.0	P	2.3	P	0.7	P	1.0 P
IL-2	m16762	1.0 A	391.4	P	1.2	A	12.3	P	1.3	A	1.0 A	23.4	P	0.2	A	1.0	A	0.3 A
IL-2	K02292	1.0 A	129.6	P	0.6	A	32.8	A	1.1	A	1.0 A	16.1	A	0.7	A	10.7	A	1.5 A
GM-CSF	X03020	1.0 P	38.0	P	0.4	A	4.1	P	0.1	A	1.0 A	15.7	P	1.4	A	2.7	A	2.1 A
IL-4	X03532	1.0 P	276.8	P	2.5	P	47.3	P	0.2	A	1.0 A	364.9	P	35.1	P	38.8	P	4.7 P
IL-4	M25892	1.0 P	38.2	P	0.2	P	7.7	P	0.1	A	1.0 P	69.6	P	7.6	P	9.1	P	1.1 P
IL-4	X03532	1.0 A	34.8	P	3.9	A	9.4	A	1.9	A	1.0 A	2.2	A	4.2	A	1.1	A	0.7 A
IL-13	M23504	1.0 A	993.0	P	1.4	A	56.1	P	1.8	A	1.0 A	140.7	P	12.3	A	19.1	A	2.3 A
TNF-α	D84196	1.0 P	30.8	P	2.1	P	1.7	P	1.2	P	1.0 P	16.5	P	2.5	P	1.8	P	2.6 P
Lymphotoxin A	M16819	1.0 P	6.9	P	0.2	A	1.4	P	0.1	A	1.0 P	2.5	P	1.7	P	1.2	P	0.9 P
IL-1α	M14639	1.0 P	25.1	P	5.6	P	3.1	P	4.4	P	1.0 P	6.7	P	5.8	P	1.1	P	2.7 P
IL-1β	M15131	1.0 P	8.0	P	9.8	P	1.3	P	7.9	P	1.0 P	3.3	P	2.2	P	0.6	P	1.5 P
*IL-1*RA	L32838	1.0 P	10.9	P	15.2	P	1.1	A	11.3	P	1.0 P	5.3	P	28.0	P	0.9	P	23.4 P
IL-3	K01668	1.0 A	33.2	P	2.6	A	4.7	A	1.2	A	1.0 A	4.0	A	1.1	A	1.4	A	1.7 A
IL-6	X54542	1.0 A	34.8	P	16.5	P	8.8	P	10.7	P	1.0 A	19.1	P	17.8	P	1.8	A	12.2 A

Real-time PCR analyses were conducted for *IFN-γ* and *IL-4* as well as for other selected cytokine genes listed in Figure 4 (data not shown) to confirm the correlation with those obtained from microarray analysis. Each probe was assigned a "call" of present (P; expressed) or "absent" (A; not expressed) using the Affymetrix decision matrix. GenBank, GenBank accession number; *IL-1*RA, *IL-1* receptor antagonist.

recently been shown to induce Th1-type activity superior to that induced by αGC, and IL-12 is indispensable for the Th1-skewing effect of the analog (27), indicating the importance of IL-12 in augmenting IFN-γ production in vivo (14, 28). Interestingly, the C-glycoside analog induces production of IFN-γ and IL-4 by NKT cells less strongly than does αGC at 2 hours after in vivo administration. Given that αGC and C-glycoside analog have the same structure for their lipid tails, they might be expected to have comparable affinity for CD1d molecules, and the slightly "twirled" α-anomeric galactose moiety between C-glycoside and O-glycoside may modulate the agonistic effect of these glycolipids. Furthermore, the C-glycoside is more resistant to hydrolysis in vivo and may have an advantage for effective production of IL-12 by APCs. In fact, OCH induces marginal IL-12 production after in vivo administration (data not shown), which makes it unable to induce IFN-γ production by various cells. Therefore, the beneficial feature of OCH as an immunomodulator is that it does not trigger production of IFN-γ in vivo.

As described previously, NKT cells recognize glycolipid antigens in the context of the nonpolymorphic MHC class I-like molecule CD1d (4). Crystal structure analysis revealed that the mouse CD1d molecule has a narrow and deep binding groove with extremely hydrophobic pockets, A′ and F′ (29). Thus the two aliphatic hydrocarbon chains would be captured by this binding groove of CD1d and the more hydrophilic galactose moiety of αGC or OCH would be presented to TCR on NKT cells. As OCH is an analog of αGC with a truncated sphingosine chain, it could be predicted that truncation of the hydrocarbon chain would make it more unstable on CD1d, which might then affect the duration of TCR stimulation on NKT cells. We demonstrated in this study that OCH detached from the CD1d molecule more rapidly than did αGC after a short-term pulse in which the glycolipids were segregated from the endosomal/lysosomal pathway. Accordingly, we showed that the initiation of IFN-γ production by NKT cells required more prolonged TCR stimulation than was required for IL-4 production. Methods such as surface plasmon resonance were not appropriate for direct assessment of the interaction between glycolipids and CD1d, possibly because of unpredictable micelle formation and the poor solubility of glycolipids in aqueous solvents (30). The half-life of the interaction of glycolipids and CD1d was reported to be less than 1 minute by surface plasmon resonance (31), contradicting functional assays suggesting a much longer half-life. Therefore, we applied a biological assay to evaluate the stability of these glycolipids on CD1d molecules, as described previously (13).

The characteristics of OCH are somewhat analogous to those of an altered peptide ligand (APL) that has been shown to induce a subset of functional responses observed in intact peptide and, in some cases, induce production of selected cytokines by T cells (32–34). Thus, OCH and possibly other αGC derivatives could be called "altered glycolipid ligands" (AGLs). Although the biological effects of APLs and AGLs could mediate a series of similar molecular events in target cells, it should be noted that APLs and AGLs differ in their "conceptual features." That is, APLs are usually altered in their amino acid residues to modify their affinity for TCRs, whereas AGLs have truncation of their hydrocarbon chain responsible for CD1d anchoring. This paper has highlighted the duration of NKT cell stimulation by CD1d-associated glycolipids as being a critical factor for determining the nature of AGLs for selective induction of cytokine production by NKT cells.

Given that IL-4 secretion consistently precedes IFN-γ production by NKT cells after TCR ligation, we speculated there were critical differences in the upstream transcriptional requirements for the *IFN-γ* and *IL-4* genes in NKT cells. In support of this speculation, CHX treatment specifically inhibited the transcription of *IFN-γ* but not that of *IL-4*. In contrast, transcription of both cytokines was abolished by CsA treatment, indicating that TCR-mediated activation of NF-AT is essential for the production of both cytokines. TCR signal–induced NF-AT activation occurs promptly corresponding to calcium influx (35). Meanwhile, the protein expression of specific

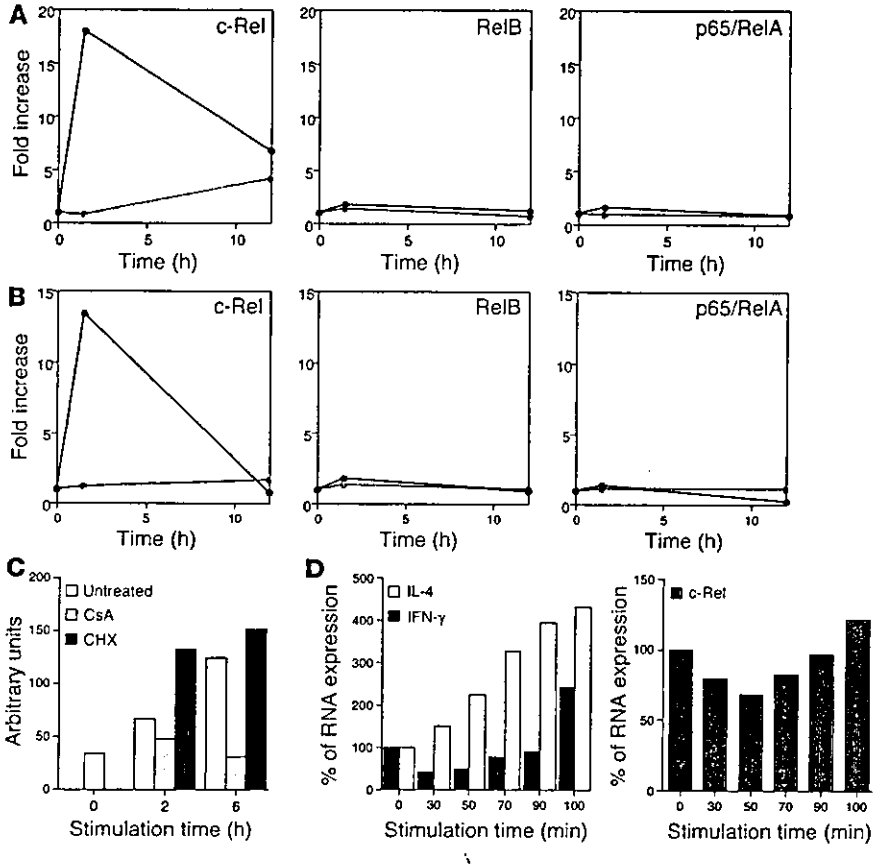

Figure 5
Induction of NF-κB family members in activated NKT cells. (**A**) Plotted values represent data of Affymetrix microarray analysis for the indicated genes.The αGC-stimulated (red lines) or OCH-stimulated (green lines) cells as well as unstimulated liver NKT cells were analyzed at the same time points and the data are presented as the relative value for stimulated NKT cells when the value in NKT cells derived from untreated animals was defined as 1. (**B**) Real-time PCR analysis for the same genes as in **A**. Data are presented as described in Figure 4. (**C**) Sorted liver NKT cells were pretreated with CsA or CHX and were stimulated with immobilized mAb to CD3, and comparative values of c-Rel transcripts relative to GAPDH were determined. (**D**) Sorted liver NKT cells were stimulated with immobilized mAb to CD3 for the indicated periods of time and then were cultured without stimulation for up to a total of 120 minutes after the initial stimulation. Total RNA was extracted from each sample and analyzed for relative amounts of transcripts of *IFN-γ* or *IL-4* (left), or *c-Rel* (right). The amount of RNA derived from unstimulated NKT cells was defined as 100%.

transcription factors takes more time to accomplish. The requirement for prolonged TCR stimulation for initiation of *IFN-γ* transcription may be due to its dependency on specific gene expression.

Recently, Matsuda et al. have shown using cytokine reporter mice that Vα14-invariant NKT cells express cytokine transcripts in the resting state, but express protein only after stimulation (22). We obtained a similar result with our microarray analysis, in that many cytokine transcripts including *IFN-γ* and *IL-4* were detectable in unstimulated NKT cells derived from liver or spleen, because most of them were assigned a "call" of "present" by the Affymetrix decision matrix, which means they were significantly expressed. The mechanism of translation of pre-existing cytokine transcripts after activation of NKT cells remains to be investigated.

Through microarray analysis and real-time PCR, we next identified a member of the NF-κB family of transcription factors, c-Rel, as being a protein rapidly expressed after αGC treatment and possibly responsible for the transcription of *IFN-γ*. Treatment with αGC selectively upregulated *c-Rel* transcription 1.5 hours after stimulation of NKT cells in vivo. OCH treatment, however, showed no induction of *c-Rel* transcription. Although *c-Rel* is transcriptionally upregulated after TCR stimulation of T cells (36), transcription of other NF-κB family members such as *p65/RelA*, *RelB*, *NF-κB1*, and *NF-κB2* was unchanged (data not shown). CsA treatment inhibited c-Rel transcription, but CHX did not, indicating that inducible transcription of c-Rel was directly controlled by TCR signal-mediated activation of NF-AT, which is consistent with a previous report (19). Although the pre-existing NF-κB proteins in general provide a means of rapidly altering cellular responses by inducing the destruction of IκB in order to enable NF-κB to be free for nuclear translocation and DNA binding, most of the nuclear c-Rel induced after T cell stimulation has been shown to be derived from newly translated c-Rel proteins. In contrast, pre-existing c-Rel scarcely translocates to the nucleus at all (36), indicating that the nuclear induction of c-Rel in T lymphocyte requires ongoing protein synthesis. The retrovirally transduced loss-of-function mutant c-Rel (c-RelΔTA) significantly inhibited transcription of *IFN-γ* genes, indicating the crucial role of c-Rel in their transcription after activation of NKT cells. Although it is possible that the Rel domain of the dominant negative mutant may affect a number of NF-κB dimers, it is unlikely, because IFN-γ production by stimulated NKT cells were CHX sensitive and other NK-κB members were not induced after stimulation in the microarray analysis. Retroviral transduction of wild-type c-Rel into NKT cells resulted in slightly augmented expression of IFN-γ after stimulation. Induction of endogenous c-Rel after in vitro stimulation might reduce the effect of retrovirally introduced c-Rel protein.

Whereas c-Rel has been associated with the functions of various cell types, its role in the immune system was first demonstrated in its involvement in *IL-2* transcription (37), in which it possibly induced chromatin remodeling of the promoter (38). Recently, the promoters for the genes encoding *IL-3*, *IL-5*, *IL-6*, *TNF-α*, *GM-CSF*, and *IFN-γ* were shown to contain κB sites or the κB-related CD28RE. Gene targeting of *c-Rel* in mice revealed that *c-Rel*–deficient T cells have a defect in the production of IL-2, IL-3, IL-5, GM-CSF, TNF-α, and IFN-γ, although expression of some of the cytokines was rescued by the addition of exogenous IL-2 (39, 40). Regarding the involvement of c-Rel in IFN-γ production, the c-Rel inhibitor pentoxyfylline (41) selectively suppresses Th1 cytokine production and EAE induction (42), and transgenic mice expressing the *trans*-dominant form of IκBα have a defect in IFN-γ production and the Th1 response (43). Recently, an elegant study using *c-Rel*–deficient mice revealed *c-Rel* has crucial roles in IFN-γ production by activated T cells and conse-

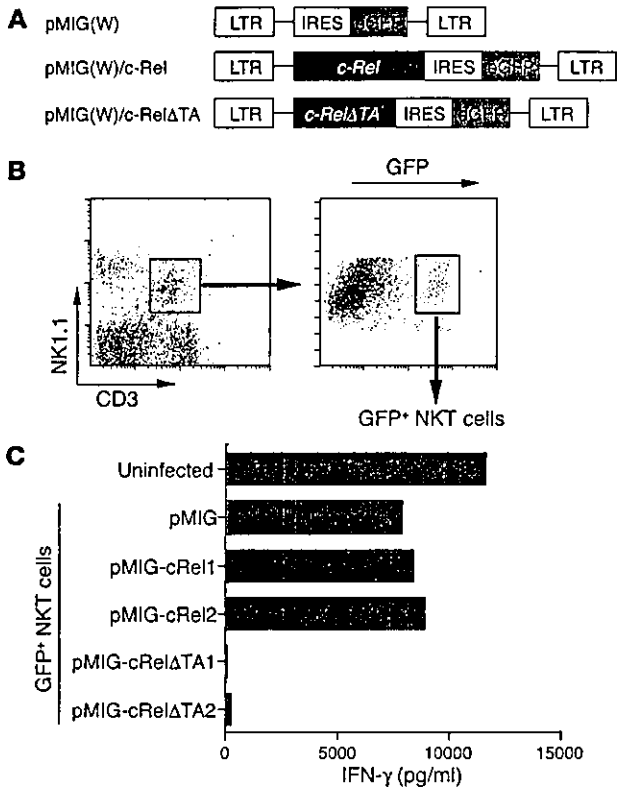

Figure 6
Cytokine production after retroviral transduction of c-Rel or c-RelΔTA into NKT cells. (**A**) DNA fragments encoding wild-type c-Rel or its mutant were cloned into the pMIG(W) bicistronic retrovirus vector. The mutant form of c-Rel (c-RelΔTA) lacks the transactivation domain of the c-Rel protein. LTR, long terminal repeat; IRES, internal ribosome entry site; eGFP, enhanced GFP. (**B**) Flow cytometric identification of cells transfected with the viral vector. Among the NK1.1$^+$CD3$^+$ liver NKT cells identified in the left panel, approximately 10% were GFP positive. The GFP-positive NKT cells were sorted for further analysis. (**C**) IFN-γ production by NKT cells transfected with c-Rel or its dominant negative mutant. The CD3$^+$NK1.1$^+$ NKT cells infected with the viruses were isolated based on their expression of GFP and were stimulated with immobilized mAb to CD3. For transduction of c-Rel or c-RelΔTA into NKT cells, two independent clones of each retroviral vector were used. The level of IFN-γ in the supernatants was measured by ELISA.

quent Th1 development by affecting the cellular functions of both T cells and APCs (20).Thus, the critical involvement of c-Rel for IFN-γ production in NKT cells is consistent with these findings.

Our results indicate that rapid calcium influx and subsequent NF-AT activation is essential for IFN-γ production by activated NKT cells and that c-Rel plays a crucial role in IFN-γ production as well. NF-AT shows quick and sensitive nucleocytoplasmic shuttling after TCR activation (35). Feske et al. demonstrated that the pattern of cytokine production by T cells was determined by the duration of nuclear residence of NF-AT (44) and that sustained NF-AT signaling promoted IFN-γ expression in CD4$^+$ T cells (45). Considering the structural feature of αGC with longer lipid chain, sustained stimulation by αGC induces long-lasting calcium influx, resulting in sustained nuclear residence of NF-AT, and c-Rel protein synthesis, which enables NKT cells to produce IFN-γ. In contrast, the rather sporadic stimulation by OCH induces short-lived nuclear residence of NF-AT, followed by marginal c-Rel expression, which leaves NKT cells unable to produce IFN-γ (Figure 7). Thus, the kinetic and quantitative differences between αGC and OCH in the induction of transcription factors, such as NF-AT and c-Rel, determine the pattern of cytokine production by NKT cells. As CD1d molecules are nonpolymorphic and are remarkably well conserved among the species, the preferential induction of IL-4 production through NKT activa-

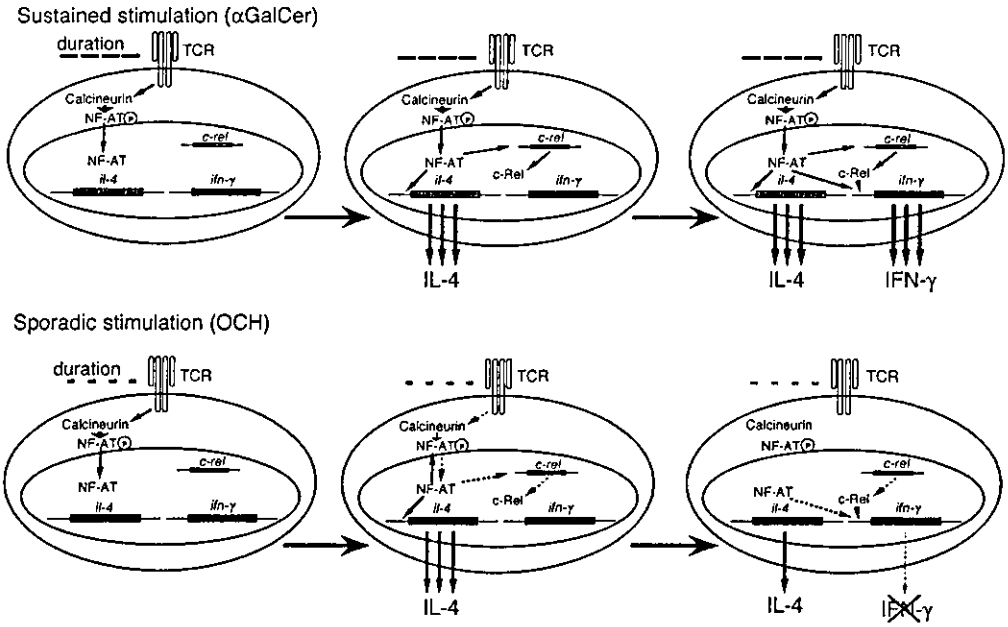

Figure 7
A model for the differential expression of IFN-γ and IL-4 after treatment of NKT cells with αGC or OCH. See text for details.

tion and subsequent Th2 polarization suggest that OCH may be an attractive therapeutic reagent to use for Th1-mediated autoimmune diseases such as multiple sclerosis and rheumatoid arthritis.

Acknowledgments

We thank Kyoko Hayakawa and Sebastian Joyce for providing the cell lines; Thomas Grundström for providing the c-Rel plasmid; and Luk Van Parijs for providing the retroviral vectors and packaging vector. We also thank Miho Mizuno and Chiharu Tomi for excellent technical assistance; and Yuki Kikai for cell sorting. We are grateful to John Ludvic Croxford for critical reading of the manuscript. This work was supported by the Organization for Pharmaceutical Safety and Research, Grant-in-Aid for Scientific Research (B) 14370169 from Japan Society for the Promotion of Science, Mochida Memorial Foundation, and Uehara Memorial Foundation.

Received for publication December 18, 2003, and accepted in revised form April 6, 2004.

Address correspondence to: Sachiko Miyake, Department of Immunology, National Institute of Neuroscience, NCNP, 4-1-1 Ogawahigashi, Kodaira, Tokyo 187-8502, Japan. Phone: 81-42-341-2711; Fax: 81-42-346-1753; E-mail: miyake@ncnp.go.jp.

1. Kronenberg, M., and Gapin, L. 2002. The unconventional lifestyle of NKT cells. *Nat. Rev. Immunol.* 2:557-568.
2. Taniguchi, M., Harada, M., Kojo, S., Nakayama, T., and Wakao, H. 2003. The regulatory role of Vα14 NKT cells in innate and acquired immune response. *Annu. Rev. Immunol.* 21:483-513.
3. Brossay, L., et al. 1998. CD1d-mediated recognition of an α-galactosylceramide by natural killer T cells is highly conserved through mammalian evolution. *J. Exp. Med.* 188:1521-1528.
4. Kawano, T., et al. 1997. CD1d-restricted and TCR-mediated activation of vα14 NKT cells by glycosylceramides. *Science.* 278:1626-1629.
5. Spada, F.M., et al. 1998. CD1d-restricted recognition of synthetic glycolipid antigens by human natural killer T cells. *J. Exp. Med.* 188:1529-1534.
6. Carnaud, C., et al. 1999. Cross-talk between cells of the innate immune system: NKT cells rapidly activate NK cells. *J. Immunol.* 163:4647-4650.
7. Fujii, S.I., Shimizu, K., Smith, C., Bonifaz, L., and Steinman, R.M. 2003. Activation of natural killer T cells by α-galactosylceramide rapidly induces the full maturation of dendritic cells in vivo and thereby acts as an adjuvant for combined CD4 and CD8 T cell immunity to a coadministered protein. *J. Exp. Med.* 198:267-279.
8. Chiba, A., et al. 2004. Suppression of collagen-induced arthritis by natural killer T cell activation with OCH, a sphingosine-truncated analog of α-galactosylceramide. *Arthritis Rheum.* 50:305-313.
9. Miyamoto, K., Miyake, S., and Yamamura, T. 2001. A synthetic glycolipid prevents autoimmune encephalomyelitis by inducing TH2 bias of natural killer T cells. *Nature.* 413:531-534.
10. Burdin, N., et al. 1998. Selective ability of mouse CD1 to present glycolipids: α-galactosylceramide specifically stimulates Vα 14+ NK T lymphocytes. *J. Immunol.* 161:3271-3281.
11. De Silva, A.D., et al. 2002. Lipid protein interactions: the assembly of CD1d1 with cellular phospholipids occurs in the endoplasmic reticulum. *J. Immunol.* 168:723-733.
12. Antonsson, A., Hughes, K., Edin, S., and Grundstrom, T. 2003. Regulation of c-Rel nuclear localization by binding of Ca2+/calmodulin. *Mol. Cell. Biol.* 23:1418-1427.
13. Moody, D.B., et al. 2002. Lipid length controls antigen entry into endosomal and nonendosomal pathways for CD1b presentation. *Nat. Immunol.* 3:435-442.
14. Fujii, S., Shimizu, K., Kronenberg, M., and Steinman, R.M. 2002. Prolonged IFN-γ-producing NKT response induced with α-galactosylceramide-loaded DCs. *Nat. Immunol.* 3:867-874.
15. Akbari, O., et al. 2003. Essential role of NKT cells producing IL-4 and IL-13 in the development of allergen-induced airway hyperreactivity. *Nat. Med.* 31:31.
16. Heller, F., Fuss, I.J., Nieuwenhuis, E.E., Blumberg, R.S., and Strober, W. 2002. Oxazolone colitis, a Th2 colitis model resembling ulcerative colitis, is mediated by IL-13-producing NK-T cells. *Immunity.* 17:629-638.
17. Leite-de-Moraes, M.C., et al. 2002. Ligand-activated natural killer T lymphocytes promptly produce IL-3 and GM-CSF in vivo: relevance to peripheral myeloid recruitment. *Eur. J. Immunol.* 32:1897-1904.
18. Chen, H., Huang, H., and Paul, W.E. 1997. NK1.1+ CD4+ T cells lose NK1.1 expression upon in vitro activation. *J. Immunol.* 158:5112-5119.
19. Venkataraman, L., Burakoff, S.J., and Sen, R. 1995. FK506 inhibits antigen receptor-mediated induction of c-rel in B and T lymphoid cells. *J. Exp. Med.* 181:1091-1099.
20. Hilliard, B.A., et al. 2002. Critical roles of c-Rel in autoimmune inflammation and helper T cell differentiation. *J. Clin. Invest.* 110:843-850. doi:10.1172/JCI200215254.
21. Carrasco, D., et al. 1998. Multiple hemopoietic defects and lymphoid hyperplasia in mice lacking the transcriptional activation domain of the c-Rel protein. *J. Exp. Med.* 187:973-984.
22. Matsuda, J.L., et al. 2003. Mouse Vα14i natural killer T cells are resistant to cytokine polarization in vivo. *Proc. Natl. Acad. Sci. U. S. A.* 100:8395-8400.
23. Tsytsykova, A.V., Tsirtsikov, E.N., and Geha, R.S. 1996. The CD40L promoter contains nuclear factor of activated T cells-binding motifs which require AP-1 binding for activation of transcription. *J. Biol. Chem.* 271:3763-3770.
24. Parra, E., Mustelin, T., Dohlsten, M., and Mercola, D. 2001. Identification of a CD28 response element in the CD40 ligand promoter. *J. Immunol.* 166:2437-2443.
25. Kitamura, H., et al. 1999. The natural killer T (NKT) cell ligand α-galactosylceramide demonstrates its immunopotentiating effect by inducing interleukin (IL)-12 production by dendritic cells and IL-12 receptor expression on NKT cells. *J. Exp. Med.* 189:1121-1128.
26. Smyth, M.J., et al. 2002. Sequential production of interferon-γ by NK1.1+ T cells and natural killer cells is essential for the antimetastatic effect of α-galactosylceramide. *Blood.* 99:1259-1266.
27. Schmieg, J., Yang, G., Franck, R.W., and Tsuji, M. 2003. Superior protection against malaria and melanoma metastases by a C-glycoside analogue of the natural killer T cell ligand α-galactosylceramide. *J. Exp. Med.* 198:1631-1641.
28. Brigl, M., Bry, L., Kent, S.C., Gumperz, J.E., and Brenner, M.B. 2003. Mechanism of CD1d-restricted natural killer T cell activation during microbial infection. *Nat. Immunol.* 4:1230-1237.
29. Zeng, Z., et al. 1997. Crystal structure of mouse CD1: An MHC-like fold with a large hydrophobic binding groove. *Science.* 277:339-345.
30. Cantu, C., 3rd, Benlagha, K., Savage, P.B., Bendelac, A., and Teyton, L. 2003. The paradox of immune molecular recognition of α-galactosylceramide: low affinity, low specificity for CD1d, high affinity for αβ TCRs. *J. Immunol.* 170:4673-4682.
31. Benlagha, K., Weiss, A., Beavis, A., Teyton, L., and Bendelac, A. 2000. In vivo identification of glycolipid antigen-specific T cells using fluorescent CD1d tetramers. *J. Exp. Med.* 191:1895-1903.
32. Evavold, B.D., and Allen, P.M. 1991. Separation of IL-4 production from Th cell proliferation by an altered T cell receptor ligand. *Science.* 252:1308-1310.
33. Chaturvedi, P., Yu, Q., Southwood, S., Sette, A., and Singh, B. 1996. Peptide analogs with different affinities for MHC alter the cytokine profile of T helper cells. *Int. Immunol.* 8:745-755.
34. Boutin, Y., Leitenberg, D., Tao, X., and Bottomly, K. 1997. Distinct biochemical signals characterize agonist- and altered peptide ligand-induced differentiation of naive CD4+ T cells into Th1 and Th2 subsets. *J. Immunol.* 159:5802-5809.
35. Zhu, J., and McKeon, F. 2000. Nucleocytoplasmic shuttling and the control of NF-AT signaling. *Cell. Mol. Life Sci.* 57:411-420.
36. Venkataraman, L., Wang, W., and Sen, R. 1996. Differential regulation of c-Rel translocation in activated B and T cells. *J. Immunol.* 157:1149-1155.
37. Ghosh, P., Tan, T.H., Rice, N.R., Sica, A., and Young, H.A. 1993. The interleukin 2 CD28-responsive complex contains at least three members of the NF κ B family: c-Rel, p50, and p65. *Proc. Natl. Acad. Sci. U. S. A.* 90:1696-1700.
38. Rao, S., Gerondakis, S., Woltring, D., and Shannon, M.F. 2003. c-Rel Is required for chromatin remodeling across the IL-2 gene promoter. *J. Immunol.* 170:3724-3731.
39. Gerondakis, S., et al. 1996. Rel-deficient T cells exhibit defects in production of interleukin 3 and granulocyte-macrophage colony-stimulating factor. *Proc. Natl. Acad. Sci. U. S. A.* 93:3405-3409.
40. Kontgen, F., et al. 1995. Mice lacking the c-rel proto-oncogene exhibit defects in lymphocyte proliferation, humoral immunity, and interleukin-2 expression. *Genes Dev.* 9:1965-1977.
41. Wang, W., Tam, W.F., Hughes, C.C., Rath, S., and Sen, R. 1997. c-Rel is a target of pentoxifylline-mediated inhibition of T lymphocyte activation. *Immunity.* 6:165-174.
42. Rott, O., Cash, E., and Fleischer, B. 1993. Phosphodiesterase inhibitor pentoxifylline, a selective suppressor of T helper type 1- but not type 2-associated lymphokine production, prevents induction of experimental autoimmune encephalomyelitis in Lewis rats. *Eur. J. Immunol.* 23:1745-1751.
43. Aronica, M.A., et al. 1999. Preferential role for NF-κ B/Rel signaling in the type 1 but not type 2 T cell-dependent immune response in vivo. *J. Immunol.* 163:5116-5124.
44. Feske, S., Draeger, R., Peter, H.H., Eichmann, K., and Rao, A. 2000. The duration of nuclear residence of NFAT determines the pattern of cytokine expression in human SCID T cells. *J. Immunol.* 165:297-305.
45. Porter, C.M., and Clipstone, N.A. 2002. Sustained NFAT signaling promotes a Th1-like pattern of gene expression in primary murine CD4+ T cells. *J. Immunol.* 168:4936-4945.

A Structural Basis for the Association of DAP12 with Mouse, but Not Human, NKG2D[1]

David B. Rosen,* Manabu Araki,[2†] Jessica A. Hamerman,* Taian Chen,* Takashi Yamamura,† and Lewis L. Lanier[3]*

Prior studies have revealed that alternative mRNA splicing of the mouse *NKG2D* gene generates receptors that associate with either the DAP10 or DAP12 transmembrane adapter signaling proteins. We report that NKG2D function is normal in human patients lacking functional DAP12, indicating that DAP10 is sufficient for human NKG2D signal transduction. Further, we show that human NKG2D is incapable of associating with DAP12 and provide evidence that structural differences in the transmembrane of mouse and human NKG2D account for the species-specific difference for this immune receptor. *The Journal of Immunology,* **2004, 173: 2470–2478.**

The activity of NK cells is regulated by a balance of positive and negative signals transduced, respectively, via activating and inhibitory cell surface receptors (1, 2). The activating receptor NKG2D, a C type-like lectin and type II transmembrane (TM)[4] protein (3), is expressed on all NK cells, γδ TCR$^+$ T cells, and human CD8$^+$ T cells and is induced on activated mouse CD8$^+$ T cells (4). NKG2D recognizes several MHC-related ligands, including the UL16-binding protein and MHC class I-related chain family of proteins in humans (5, 6) and H60, RAE-1, and MULT-1 in mice (7–10). These NKG2D ligands, though usually absent from or expressed at low levels by normal adult tissues, are often induced on stressed, infected, or tumor cells in adult life (reviewed in Ref. 11). In this fashion, leukocytes expressing NKG2D can directly recognize transformed or infected cells.

Activation through NKG2D can have multiple outcomes including the production of IFN-γ and the triggering of cell-mediated cytotoxicity (5, 12). In αβ TCR$^+$ T cells, NKG2D has been suggested to provide a costimulatory role similar to CD28, enhancing TCR-mediated signaling events (13, 14). In vivo NKG2D is involved in antitumor as well as antiviral immunity (reviewed in Ref. 15).

NKG2D itself lacks intrinsic signaling capabilities. Like the TCR, NKG2D contains a positively charged amino acid within its TM region and requires association with adapter signaling proteins for cell surface expression. These adapter proteins contain complementary negatively charged amino acids within their TM regions that provide a salt bridge with NKG2D. Both in mice and humans, NKG2D homodimers associate with and signal through homodimers of the TM adapter protein DAP10 (12, 16). Signaling through DAP10 involves phosphorylation of its cytoplasmic YXXM motif, recruitment of the p85 subunit of phosphatidylinositol-3 kinase, and downstream signaling through AKT (16–18).

In mice, alternative mRNA splicing generates two functionally distinct isoforms of the NKG2D protein (12). The mouse NKG2D long (mNKG2D-L) protein comprises 232 amino acids, whereas the mouse NKG2D short (mNKG2D-S) protein lacks the first 13 N-terminal amino acids and initiates translation at a second methionine in the cytoplasmic domain of this type II protein. This shorter isoform is expressed in activated, but not resting, mouse NK cells and is capable of pairing with homodimers of either DAP10 or DAP12, an ITAM-containing TM adapter protein. Like other ITAM sequences, DAP12 intracellular YXXL$_{6-8X}$ YXXL motif recruits Syk family kinases (19). Mouse NKG2D-L pairs exclusively with DAP10 (12). Both DAP10 and DAP12 signaling contribute to NK cell-mediated cytotoxicity, whereas DAP12 signaling also definitively stimulates cytokine production, such as IFN-γ (12, 16, 20, 21).

The ability of the mouse NKG2D to generate identical receptors with distinct signaling properties by virtue of association with different adapter proteins prompted the question of whether human NKG2D also demonstrates this property. In this study, we have examined NKG2D expression and functional activity in human PBMCs of patients lacking a functional *DAP12* gene and have explored the structural basis for association of human and mouse NKG2D with the DAP10 and DAP12 adapter proteins.

Materials and Methods

Characterization of patients with Nasu-Hakola

The *DAP12* (*tyrobp*) gene in a patient with Nasu-Hakola, designated NH1, has a single base mutation in the start codon of exon 1 that has recently been identified in Japanese patients (22). Patients NH2 and NH3 have a single base deletion in exon 3 (22, 23). Loss of DAP12 protein expression in these patients was confirmed by Western blotting as previously described (22). Studies of all these subjects were conducted according to the institutional guideline.

Cytotoxicity assays

PBMC were prepared from peripheral blood samples of healthy individuals and three patients with Nasu-Hakola disease using density gradient centrifugation by using Ficoll-Hypaque Plus (Amersham Pharmacia Biotech, Uppsala, Sweden). PBMC were resuspended at 2 × 10^6/ml in RPMI 1640

*Department of Microbiology and Immunology and the Cancer Research Institute, University of California, San Francisco, CA 94143; and †Department of Immunology, National Institute of Neuroscience, National Center of Neurology and Psychiatry, Kodaira, Tokyo

Received for publication February 10, 2004. Accepted for publication June 7, 2004.

The costs of publication of this article were defrayed in part by the payment of page charges. This article must therefore be hereby marked *advertisement* in accordance with 18 U.S.C. Section 1734 solely to indicate this fact.

[1] This work was supported by The Irvington Institute for Immunological Research (to J.A.H.) and by National Institutes of Health Grant CA89189. L.L.L. is an American Cancer Society Research Professor.

[2] Current address: Center for Neurologic Diseases, Brigham and Women's Hospital, Harvard Medical School, 77 Avenue Louis Pasteur, Neuroscience Research Building Room 641, Boston, MA 02115-5817.

[3] Address correspondence and reprint requests to Dr. Lewis L. Lanier, Department of Microbiology and Immunology, University of California, 513 Parnassus Avenue, Health Sciences East Room 1001G, Box 0414, San Francisco, CA 94143-0414. E-mail address: lanier@itsa.ucsf.edu

[4] Abbreviations used in this paper: TM, transmembrane; EC, extracellular; mTM hEC, mouse-human NKG2D chimeras; IRES, internal ribosomal entry site; mCJS, murine cytoplasmic juxtamembrane sequence.

0022-1767/04/$02.00

medium supplemented with 10% FCS, 2 mM L-glutamine, HEPES, penicillin/streptomycin, and 2-ME. PBMC were plated into 24-well plates in the presence of 100 U/ml rIL-2, for mAb-induced redirected cytolytic assays, or 1000 U/ml rIL-2, for BaF/3 cytotoxicity assays rIL-2 (Shionogi, Osaka, Japan). A lower concentration of IL-2 was used for assays with P815 target cells as high doses of IL-2 cause considerable background cytotoxicity against P815, likely due to lymphokine-activated killer activity. Activated PBMC were harvested after 48-h culture, then used in 4-h ^{51}Cr release cytotoxicity assays as described (24). BaF/3, BaF/3 cells expressing MICA*0019, and FcR$^+$ P815 cells were labeled with 100 μCi of ^{51}Cr (PerkinElmer, Boston, MA) for 2 h at 37°C, washed three times, and used as target cells in cell-mediated cytotoxicity assays. For mAb-induced redirected cytotoxicity assays using P815 target cells, PBMC were cultured in the presence of medium only, control mAb anti-CD56 mAb (Leu19; BD Immunocytometry Systems, San Jose, CA) or anti-NKG2D mAb (made in collaboration with Dr. J. Houchins; R&D Systems, Minneapolis, MN). Monoclonal Abs were used at a final concentration of 2.5 μg/ml.

cDNAs, chimeras, and plasmids

Human "short" NKG2D, human truncated NKG2D, mouse truncated NKG2D, mouse-human NKG2D chimeras (mTM hEC), and NKG2D-CD69 chimeras were created by standard PCR mutagenesis. TM regions were determined by using the following TM prediction programs and a consensus sequence was obtained by comparison of the analyses: Tmap (http://srs.ebi.ac.uk/srsbin/cgi-bin/wgetz?-page+Launch+-id+1dvsK1MjgHZ+-appl+tmap+-launchFrom+top); DAS (http://www.sbc.su.se/~miklos/DAS/); Tmpred (http://www.ch.embnet.org/software/TMPRED_form.html); HMMTOP (http://www.enzim.hu/hmmtop/html/submit.html); SOSUI (http://sosui.proteome.bio.tuat.ac.jp/cgi-bin/sosui.cgi?/sosui_submit.html); and TMHMM (http://www.cbs.dtu.dk/services/TMHMM/). Protein chimeras and truncations were created using the following amino acids: mΔNKG2D begins at K48, hΔNKG2D at R47, and ΔCD69 at V39 (with numbering beginning at the first amino acid in the mNKG2D-L isoform and the human NKG2D and CD69 sequences). Mouse NKG2D TM construct consists of amino acids K48-V84 and the human NKG2D TM constructs span R47-N80. Human NKG2D extracellular (EC) construct begins at L82, and the human CD69 EC construct at G65. The human NKG2D short intracellular region construct consists of M15-E48, the human long intracellular construct of M1-E48 and the mouse NKG2D tail construct spans M1-E13. CD69 cDNA was synthesized from mRNA isolated from Jurkat T cells stimulated 24 h with 25 ng/ml PMA (Calbiochem, Darmstadt, Germany) by reverse transcription with Superscript II (Invitrogen Life Technologies, Carlsbad, CA). Site-directed mutagenesis was performed using a Quick Change kit (Invitrogen Life Technologies), according to the manufacturer's instructions. All constructs were confirmed by DNA sequencing. cDNAs were subcloned into pMx-pie (containing a puromycin resistance gene, an internal ribosomal entry site (IRES) element, and the enhanced GFP gene) or pMX-puro retroviral vectors (25).

Cells and transfectants

Plasmid constructs were transfected with Lipofectamine 2000 (Invitrogen Life Technologies) into the Phoenix packaging cell lines (generous gifts from Dr. G. Nolan, Stanford University, Palo Alto, CA) (26) to produce retroviruses. Retroviruses in medium containing 8 μg/ml polybrene (Sigma-Aldrich, St. Louis, MO) were used to infect BaF/3 reporter cells. Briefly, polybrene was added to retroviral supernatants and the mixture was used to resuspend BaF/3 reporter cells. Following centrifugation of the cells in the retrovirus-containing medium (1300 × *g* for 2.5 h), transfected reporter cells were incubated for 48 h at 37°C and then assayed for transgene expression. BaF/3 reporter cells were created from the mouse pro-B BaF/3 cell line. Dr. S. Tangye (Centenary Institute, Sydney, Australia) generously provided BaF/3 cells transfected with a mouse IL-3 cDNA to permit autocrine production of this requisite growth factor. To create Myc-DAP10 reporter cells, IL-3$^+$ BaF/3 cells were infected with retroviruses (pMX-puro vector) containing a cDNA including the human CD8 leader segment, followed by the Myc epitope (EQKLISEEDL) joined to the EC N-terminal domain of human DAP10 (27). Similarly, to create Flag-DAP12 reporter cells, IL-3$^+$ BaF/3 cells were infected with retroviruses (pMX-puro vector) containing cDNA including the human CD8 leader segment, followed by the Flag epitope (DYKDDDDK) joined to the EC N-terminal domain of human DAP12, as described (19, 28). Infected cells were then selected in RPMI 1640 medium supplemented with 10% FCS, 2 mM L-glutamine, and 1 μg/ml puromycin.

Flow cytometry and Abs

For immunofluorescence analysis of transfected *myc*-DAP10 BaF/3 reporter cells, 1 × 10^6 cells were stained with anti-*myc* mAb 9E11 (generously provided by Dr. G. Evan, University of California, San Francisco, CA), followed by a donkey anti-mouse IgG secondary Ab conjugated to PE (Jackson ImmunoResearch Laboratories, West Grove, PA). Cells were then preincubated in 10% normal mouse serum before being stained with either biotin-conjugated mouse anti-human NKG2D mAb (clone 149810, R&D Systems), biotin-conjugated rat anti-mouse NKG2D mAb CX5, or allophycocyanin-conjugated mouse anti-human CD69 mAb Leu23 (BD Pharmingen, San Diego, CA). Biotin-conjugated Abs were detected with CyChrome-conjugated or allophycocyanin-conjugated streptavidin (BD Pharmingen). For immunofluorescence analysis of transfected Flag-DAP12 BaF/3 reporter cells, 1 × 10^6 cells were stained with biotin-conjugated anti-Flag mAb M2 (Sigma-Aldrich), followed by CyChrome-conjugated streptavidin (BD Pharmingen). Cells were also stained prior with PE-conjugated mAb to mouse NKG2D (CX5), anti-human NKG2D, or anti-CD69 (Leu23; BD Pharmingen) followed by donkey anti-mouse IgG PE. Live cells were gated based on forward and side scatter profiles. Retrovirus-infected cells were gated based on GFP fluorescence. Cells were analyzed by using a FACSCaliber (BD Biosciences, San Jose, CA) or a small desktop Guava Personal Cytometer with Guava ViaCount and Guava Express software (Hayward, CA).

Immunoprecipitations and Western blots

A total of 50 × 10^6 transfected BaF/3 cells were solubilized in 1 ml Brij-Nonidet P-40 lysis buffer (0.875% Brij 97, 0.125% Nonidet P-40, 10 mM Tris base, 150 mM NaCl (pH 8.0), and protease inhibitors; all Sigma-Aldrich). Cell lysates were precleared with 60 μl of protein G-Sepharose beads (Amersham Pharmacia Biotech) for 1 h at 4°C. Anti-human NKG2D (clone 149810; R&D Systems) or isotype-matched control mAb were cross-linked to protein G beads by incubation in PBS for 30 min, followed by incubation in 10 mM dimethyl pimelimidate dihydrochloride (DMP; Pierce, Rockford, IL), 200 mM triethanolamine (Sigma-Aldrich) pH 8.2 for 45 min and extensive washing. Monoclonal Ab-coated beads were used for immunoprecipitation of precleared lysates for 3 h at 4°C. After washing, immunoprecipitates were eluted by adding nonreducing sample buffer and incubating for 30 min at room temperature. 2-ME (Sigma-Aldrich) was added, samples were boiled, and analyzed by 15% SDS-PAGE. Samples were transferred to Immobilon P membrane (Millipore, Bedford, MA), blocked and probed with goat anti-human DAP10 Ab N-17 (Santa Cruz Biotechnology, Santa Cruz, CA) or anti-human DAP12 mAb DX37 (27), followed by HRP-conjugated donkey anti-goat IgG (Amersham Pharmacia Biotech) or goat anti-mouse IgG (Amersham Pharmacia Biotech), respectively, and visualized with chemiluminescent substrate (Pierce).

Results

PBMCs from DAP12$^{-/-}$ patients display normal NKG2D function

Only the counterpart of the mNKG2D-L isoform has been described in humans and has been shown to coimmunoprecipitate with DAP10, but not DAP12 (16, 27). Nonetheless, this does not exclude a weak or indirect association between human NKG2D and DAP12 that may contribute to NKG2D receptor function in human lymphocytes. Therefore, studies were undertaken to address formally a potential role for DAP12 in human NKG2D receptor-dependent NK cell activation. Nasu-Hakola disease, also called polycystic lipomembranous osteodysplasia with sclerosing leukoencephalopathy, is a globally distributed recessively inherited disease caused by loss of function mutations in the *DAP12* (also called *tyrobp*) gene (23). In this report, we analyzed PBMC of three Japanese patients with Nasu-Hakola disease for their NKG2D-mediated cytolytic function. Each of these patients has a single point mutation in their *DAP12* gene that causes premature stop codons and results in a complete lack of detectable DAP12 protein (see *Materials and Methods*). We examined the peripheral blood CD3$^-$CD56$^+$ NK cells of these patients and found that the expression of NKG2D on the cell surface of their NK cells was indistinguishable from normal, healthy individuals (Fig. 1*a*). Previously, we reported that loss of function mutations in human *DAP12* did not affect expression of the closely linked *DAP10* gene (23); however, in this prior study NKG2D receptor-dependent functions were not directly analyzed.

To formally address the activity of the NKG2D receptor in patients lacking DAP12, we tested the ability of PBMCs from these

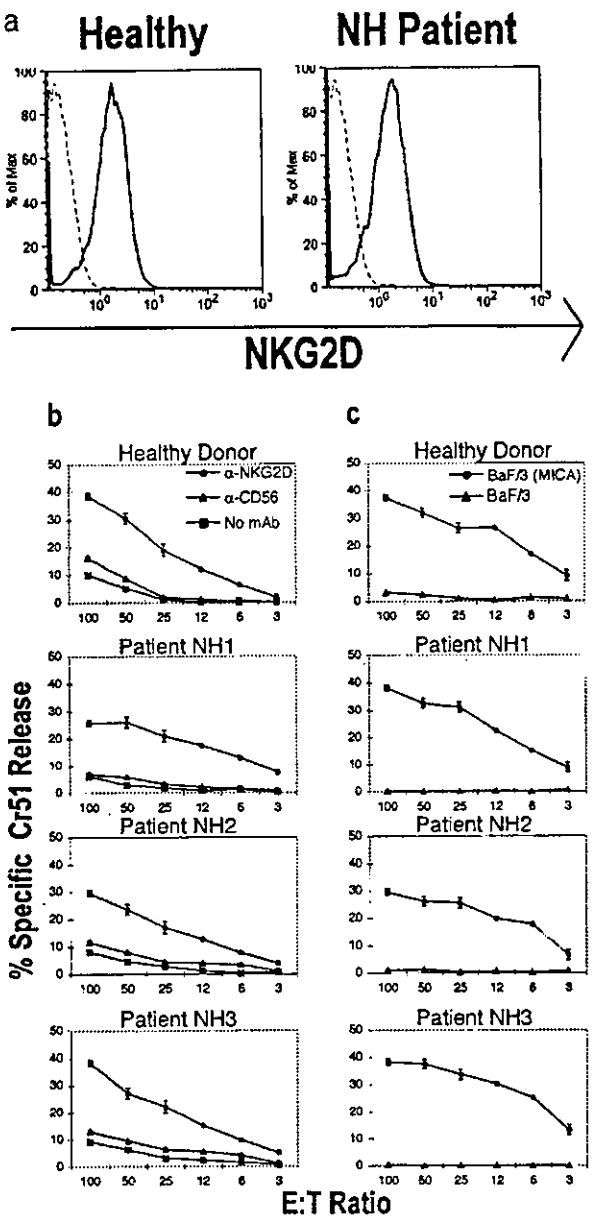

FIGURE 1. NKG2D expression and function in Nasu-Hakola patients. *a*, NKG2D levels on NK cells are identical in normal healthy humans and patients with Nasu-Hakola disease. $CD3^-CD56^+$ NK cells from PBMC of a normal, healthy individual, and Nasu-Hakola patients (NH1, NH2, and NH3) were stained with mAb against CD3, CD56, and NKG2D or appropriate control Ig and were analyzed by flow cytometry. Representative data from one Nasu-Hakola patient are shown. Isotype-matched Ig control (dashed line) and anti-NKG2D (bold lines) are shown. *b*, PBMC from a normal, healthy individual and three Nasu-Hakola patients (NH1, NH2, and NH3) were cultured for 48 h in IL-2 and assayed for mAb-induced redirected cytotoxicity against FcR^+ P815 target cells in the absence or presence of anti-NKG2D mAb or anti-CD56 mAb (used as a negative control). *c*, IL-2-activated PBMC from a normal, healthy individual, and three Nasu-Hakola patients (NH1, NH2, and NH3) were assayed for cytolytic activity against mouse Ba/F3 target cells or Ba/F3 cells stably transfected with MICA*0019, a human NKG2D ligand.

patients to kill target cells by the NKG2D-dependent pathway. This was achieved by using an anti-NKG2D mAb-induced redirected cytotoxicity assay and by using mouse target cells transfected with a human NKG2D ligand, MICA*0019. PBMCs from the three patients with Nasu-Hakola disease, as well as a normal, healthy individual, were cultured for 48 h in IL-2 and then used as effector cells in these cytotoxicity assays. Using ^{51}Cr-labeled FcR^+ P815 target cells, anti-NKG2D mAb induced cytotoxicity mediated by PBMCs of healthy individuals and patients with Nasu-Hakola disease, whereas the anti-CD56 mAb used as a negative control failed to augment lytic activity (Fig. 1*b*). No significant difference was seen in NKG2D-mediated cytotoxicity levels between the patient and control cells. To further characterize NKG2D function in patients with Nasu-Hakola disease, we performed cytotoxicity assays against BaF/3 mouse pro-B cells stably transfected with MICA*0019, a physiological ligand of human NKG2D. Although minimal cytotoxicity was seen against untransfected, parental BaF/3 cells, BaF/3 cells stably expressing MICA stimulated elevated cytotoxicity from activated PBMCs of both normal individuals and patients with Nasu-Hakola disease. No significant difference was observed in cytotoxicity levels mediated by PBMCs of healthy individuals and Nasu-Hakola patients against MICA-bearing target cells. Thus, NKG2D expression on NK cells and NKG2D-dependent functions were indistinguishable among healthy individuals and the patients with Nasu-Hakola disease. These experiments demonstrate normal human NKG2D function in the absence of DAP12.

Unlike mouse NKG2D-S, human NKG2D does not associate with DAP12

Many NK receptors, including NKG2D, KIR2DS, Ly49D, NKR-P1C, NKp30, NKp44, NKp46, and CD94/NKG2C, are multisubunit receptor complexes that convey signals via the TM adapters FcεRIγ, CD3ζ, DAP10, or DAP12 (reviewed in Ref. 29). All of these adapters have a negatively charged aspartic acid residue in their hydrophobic TM domain, which is critical for interaction with an oppositely charged basic residue in their associated ligand-binding receptors. For NKG2D, this basic residue is a conserved arginine in the TM region (Fig. 2*a*, starred residue). The human and mNKG2D-L receptors have been shown to pair and signal through DAP10, but not DAP12 (12, 16).

Recently, a second isoform of mouse NKG2D was discovered that lacks the first 13 N-terminal cytoplasmic amino acids and uses an alternative methionine start site due to alternative splicing of the transcript (12, 30). This shorter murine NKG2D isoform is capable of pairing and signaling with both DAP10 and DAP12 adapters (12, 30). Examination of the predicted amino acid sequence of human NKG2D reveals that it also contains a second N-terminal methionine residue that could potentially act as an alternative start site (Fig. 2*a*). Although to date no alternatively spliced human transcript involving the NKG2D cytoplasmic domain has been identified (31), it is impossible to exclude the existence of such isoforms at a low abundance or that they are only expressed in certain conditions of activation or in selected cell types. Therefore, we have addressed the issue using a different approach. In this model, we ask whether a theoretical short human NKG2D isoform lacking the first 14 amino acids could be able to pair with DAP12.

To address this experimentally, we artificially created a short human NKG2D using the second methionine residue as the start site and tested its ability to pair with DAP10 and DAP12. For these assays, we used mouse BaF/3 reporter cells stably transfected with Myc epitope-tagged human DAP10 or with Flag epitope-tagged human DAP12. In the absence of an associated receptor, Myc-DAP10 and FLAG-DAP12 were expressed at only low levels on the cell surface of the reporter cells. These reporter cells were infected with retroviruses encoding the wild-type human NKG2D (in our study designated as hNKG2D-L), the artificially created

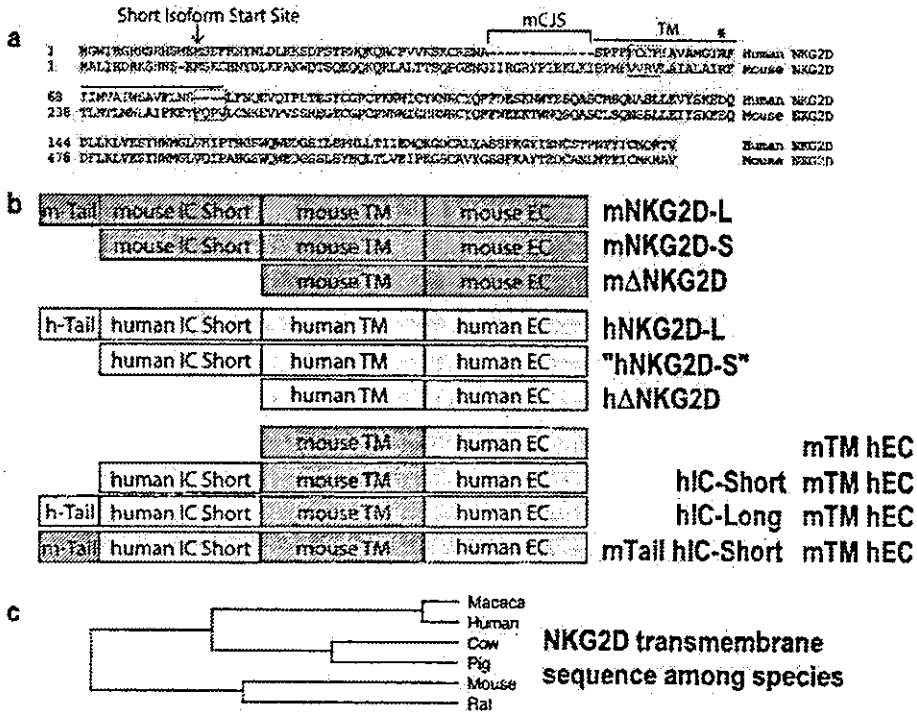

FIGURE 2. Human and mouse NKG2D comparisons and receptor constructs. *a*, Alignment of predicted mouse and human NKG2D amino acid sequences. Identical residues (shaded) in the mouse and human proteins are shown. An arrow indicates the methionine (M) beginning of the mouse NKG2D-short isoform and the artificial human "NKG2D-Short" protein. The mCJS (brackets) present in mouse, but not human, NKG2D is shown. The putative TM region (overlined) is starred to indicate the conserved arginine (R) residue required for association with DAP10 (16). Putative TM regions were defined as the consensus from six TM prediction programs (see *Materials and Methods*). Regions and residues (boxed) of interest are shown. *b*, Schematic representation is shown of the truncations and chimeric proteins generated, with the boundaries as defined in *Materials and Methods*. *c*, Phylogenetic comparison of the TM regions of NKG2D in the indicated species, as determined by Clustal W analysis of the proteins using MegAlign (DNASTAR Software, Madison, WI).

human "short" NKG2D (or hNKG2D-S), mNKG2D-L, and mNKG2D-S or an empty retroviral vector. The pMX-pie retroviral vector used in these experiments harbors an IRES-GFP element downstream of the inserted cDNA, allowing for infected cells to be readily detected by the expression of green fluorescence.

Cells were stained with mAbs against the appropriate epitope tags and either human or mouse NKG2D. Infected cells, detected by gating on GFP-positive cells using flow cytometry, were then analyzed for coexpression of NKG2D and the epitope-tagged adapter protein of interest. Coordinate expression of NKG2D and its associated adapter protein on the surface of transfected cells is indicated by the "diagonal" relationship observed in the bivariate dot plots. The long NKG2D proteins of both species and the mNKG2D-S protein paired with DAP10, as would be expected

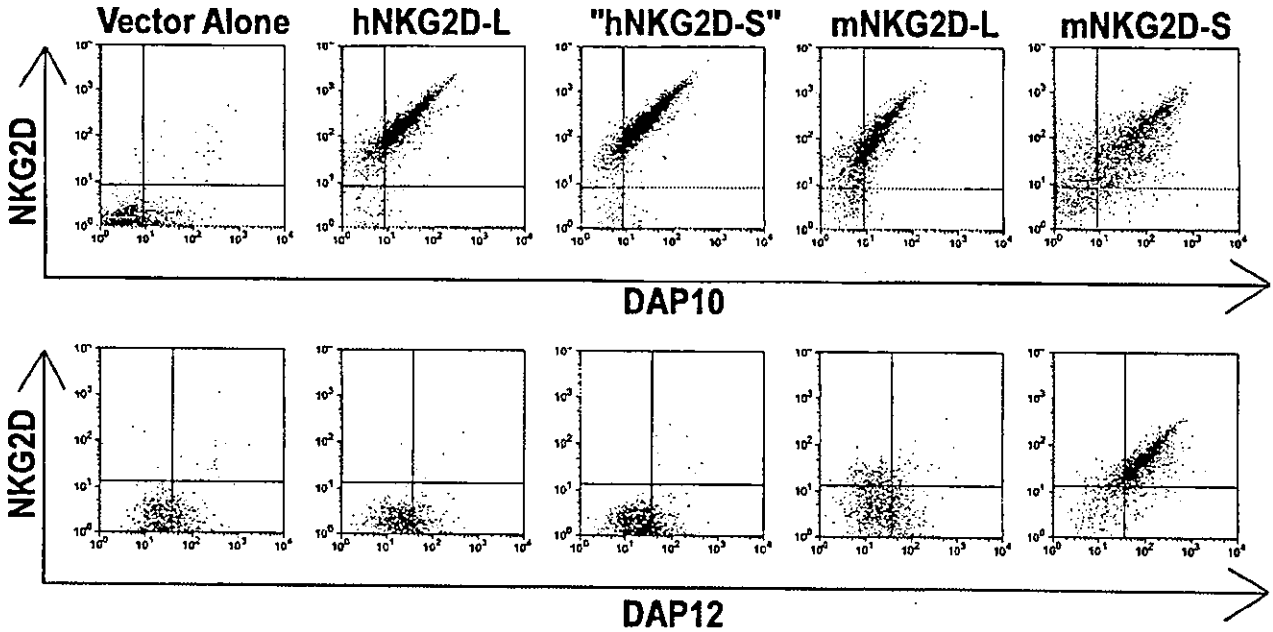

FIGURE 3. Unlike mNKG2D-S, human short NKG2D does not pair with DAP12. Ba/F3 reporter cells stably expressing Myc-DAP10 (*upper panels*) or Flag-DAP12 (*lower panels*) were infected with retroviruses with the indicated NKG2D constructs in a vector containing an IRES-GFP element. Samples were stained with the relevant anti-NKG2D and anti-epitope tag mAbs and analyzed by flow cytometry. Data shown are gated on GFP$^+$ cells, which confirmed expression of the construct in the infected cells. Results shown are representative of at least three independent experiments.

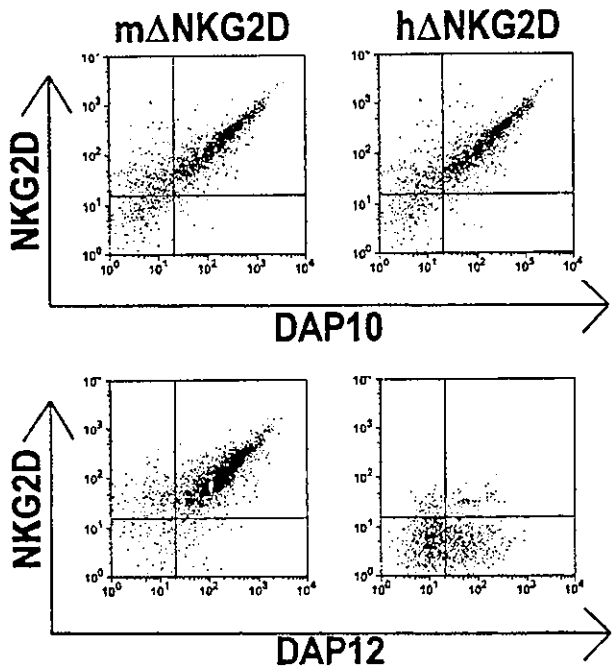

FIGURE 4. Mouse NKG2D TM and EC domains are sufficient for DAP12 association. Ba/F3 reporter cells stably expressing Myc-DAP10 or Flag-DAP12 were infected with retroviruses with the indicated NKG2D constructs, as shown in Fig. 2*b*, in a vector containing an IRES-GFP element. Samples were stained with the relevant anti-NKG2D and anti-epitope tag mAbs and analyzed by flow cytometry. Results shown are representative of at least three independent experiments.

based on prior reports (12, 16) (Fig. 3). In accordance with prior findings (12, 30), mNKG2D-S efficiently paired with DAP12. By contrast, although the human short NKG2D associated with DAP10, it was completely unable to pair with DAP12. Human and mouse NKG2D-L were able to pair interchangeably with either human or mouse DAP10, without species preference (data not shown). Similarly, mNKG2D-S associated equally with mouse or human DAP12, whereas human short NKG2D failed to assemble with either mouse or human DAP12. Collectively, these results demonstrate a fundamental difference between the human and mouse NKG2D proteins, rather than species-specific differences in the conserved adapter proteins.

Mouse NKG2D cytoplasmic domain is not required for DAP12 association

In mouse NKG2D, the 13 amino acid N-terminal cytoplasmic tail present in mNKG2D-L, absent in mNKG2D-S, abrogates DAP12 binding (12). Similar to mouse NKG2D, the first 14 amino acids of human NKG2D preceding the second methionine in the cytoplasmic domain is a highly charged region (isoelectric point pH 12). As our artificial human short NKG2D also lacks this potentially inhibitory sequence, and is still unable to pair with DAP12, other structural elements must explain the difference between human and mouse NKG2D with respect to association with DAP12. By comparison of mouse and human NKG2D (Fig. 2), one explanation lies in a 13 amino acid stretch present in mouse, but not human NKG2D, in the cytoplasmic juxtamembrane region. This unique murine cytoplasmic juxtamembrane sequence (mCJS), designated in Fig. 2*a*, might provide a positive signal for DAP12 association, as this sequence is present in mouse but not human NKG2D. To address this possibility, we created two N-terminal truncations of mouse NKG2D: one that contained the mCJS and another that only contained the TM and EC domains (mΔNKG2D). Similarly, we created a truncated human NKG2D, which contained only the TM and EC domains (hΔNKG2D) (Fig. 2*b*). Retroviruses encoding mΔNKG2D and hΔNKG2D were used to infect Myc-DAP10 or Flag-DAP12 reporter Ba/F3 cells, as previously described.

Ab staining for the appropriate epitope tags and NKG2D revealed that mΔNKG2D was capable of pairing with both DAP10 and DAP12 (Fig. 4). This result suggests that the mCJS region is not required for DAP12 association and that the mouse NKG2D TM and EC domains are sufficient for DAP12 association. The same experiment with a truncated mouse NKG2D still containing the mCJS did not significantly improve DAP12 association, suggesting that this sequence plays no major role in DAP12 association (data not shown). Like human short NKG2D, hΔNKG2D was still able to pair with DAP10, but was incapable of pairing with DAP12. This excluded the possibility that the inability of human NKG2D to pair with DAP12 was due to an inhibitory sequence present in the cytoplasmic region. Furthermore, these results suggest that the difference between mouse and human NKG2D, with respect to DAP12 association, must lie within the TM and/or EC domains.

The mouse NKG2D TM sequence allows human NKG2D to pair with DAP12

Previous studies with a chimeric protein composed of the DAP10 EC-DAP12 TM-DAP10 cytoplasmic domains suggested a nonpermissive interaction between the TM regions of DAP12 and human NKG2D (27). Furthermore, examination of the protein sequences of human and mouse NKG2D reveals significant sequence divergence within the TM region (Fig. 2*a*, underlined). These observations spurred the question of whether the difference in DAP12 pairing ability between mouse and human NKG2D could be attributed to their TM regions. To test the hypothesis that the mouse NKG2D TM is permissive for DAP12 association whereas the human NKG2D TM is not, we created a chimeric NKG2D construct containing the mTM hEC domain (Fig. 2*b*) and tested its ability to pair with DAP10 and DAP12 in Ba/F3 reporter cells, as previously described. We found that replacing the human TM with the mouse TM region allowed the chimeric protein to stabilize expression of human DAP12 on the cell surface of the transfectants (Fig. 5*a*). In other words, the mouse NKG2D TM permitted the chimeric receptor to associate with DAP12. This conclusion was further supported by the ability to coimmunoprecipitate both DAP10 and DAP12 with the chimeric receptor containing the mouse NKG2D TM region (Fig. 5*c*). By contrast, as reported previously, human NKG2D coimmunoprecipitates with DAP10, but not with DAP12 (27, 31). These results suggest a critical difference between the TM domains of human and mouse NKG2D such that human NKG2D is not permissive for DAP12 pairing whereas mouse NKG2D is permissive.

In these experiments, we also tested whether the FQPV motif (Fig. 2*a*, boxed) on the EC membrane-proximal side of the mouse TM was necessary for DAP12 interaction, as this motif is absent from human NKG2D. Our experiments suggest this motif is unnecessary as chimeric mTM hEC proteins with or without this sequence associate equivalently with DAP12 (data not shown).

The human NKG2D cytoplasmic domain when associated with the mouse NKG2D TM region is permissive for DAP12 association

Like the mouse NKG2D 13 amino acid tail, the N-terminal portion of human NKG2D-L contains multiple charged amino acid residues (Fig. 2*a*). Because of this similarity, it is possible that the

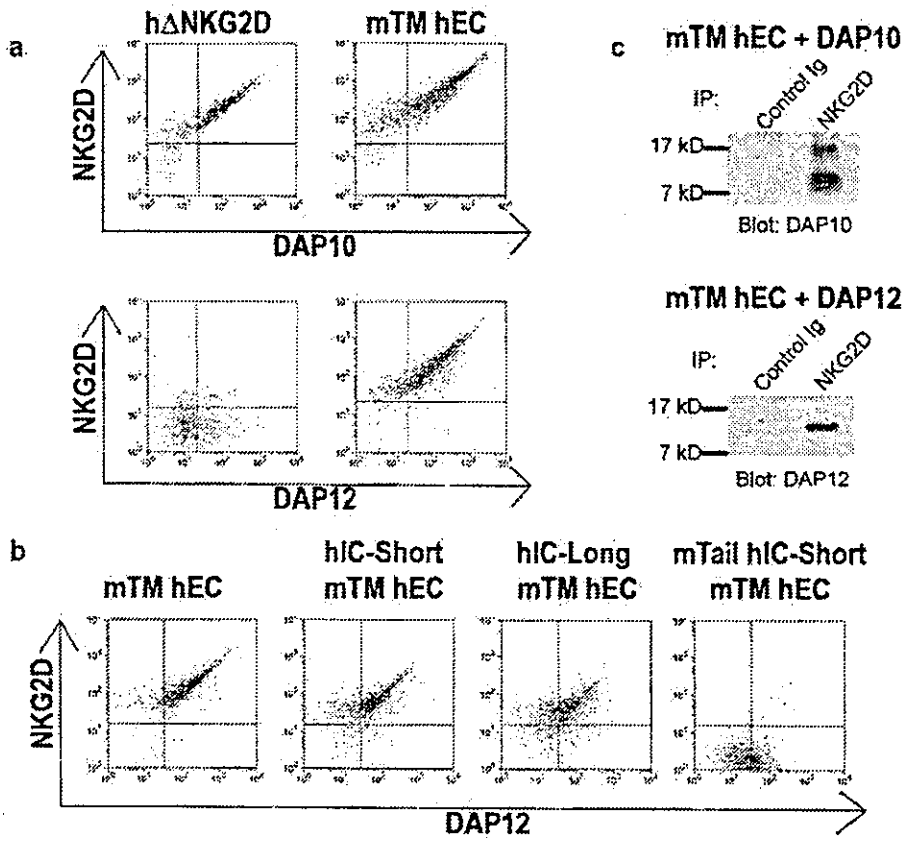

FIGURE 5. The mouse NKG2D TM region conveys DAP12 specificity to human NKG2D. *a* and *b*, Ba/F3 reporter cells stably expressing Myc-DAP10 or Flag-DAP12 were infected with retroviruses with the indicated NKG2D constructs, as shown in Fig. 2*b*, in a vector containing an IRES-GFP element. Samples were stained with the relevant anti-NKG2D and anti-epitope tag mAbs and analyzed by flow cytometry. *c*, mTM hEC chimeric NKG2D receptor coimmunoprecipitates with DAP10 and DAP12. Transfected mTM hEC reporter cells (*a*) were lysed in Brij-Nonidet P-40 lysis buffer. The receptor complexes were immunoprecipitated from lysates with anti-human NKG2D or isotype-matched control mAb. Samples were analyzed by SDS-PAGE and transferred to Immobilon P membrane and probed with goat anti-DAP10 antisera N-17 or anti-DAP12 mAb DX37, followed by HRP-conjugated donkey anti-goat IgG or goat anti-mouse IgG, respectively, and visualized with chemiluminescent substrate. As described previously (16), the heterogeneous migration pattern of DAP10 is likely due to *O*-linked glycosylation of its EC domain.

human tail behaves like the mouse tail and may also be repulsive to DAP12 association. Thus, in addition to having a nonpermissive TM region in human NKG2D, the repulsive segment present in mNKG2D-L cytoplasmic domain might have been conserved in humans to prevent potential association with DAP12. To answer the question of whether the long cytoplasmic domains of human NKG2D or the artificial "short" hNKG2D are permissive for DAP12 binding, we created NKG2D chimeras from the mTM-hEC construct adding back the human "short" intracellular domain (hIC-"Short" mTM hEC), the human long intracellular domain (hIC-Long mTM hEC), or the human "short" intracellular domain with the mouse N-terminal 13-aa tail (mTail hIC-"Short" mTM hEC), as portrayed graphically in Fig. 2*B*. As expected, all of these chimeric constructs paired with DAP10 (data not shown).

Using retroviral infection of the Flag-DAP12 reporter BaF/3 cells, we found that the entire human intracellular domain, in both the artificial short and natural long isoforms, failed to prevent DAP12 association when the TM region of mNKG2D is present in the chimeric receptors (Fig. 5*b*). In contrast, addition of the mouse tail to the human short intracellular domain abrogated DAP12 association. These results demonstrate that the N-terminal tail sequence of mouse NKG2D is necessary to prevent association of DAP12 with the mNKG2D-L isoform. This repulsion cannot be due to charge alone because the N-terminal segments of both mouse and human NKG2D are rich in acidic and basic amino acid residues. From an evolutionary perspective, mouse NKG2D may have evolved a repulsive tail and alternative splicing of NKG2D as mechanisms to regulate DAP12 adapter signaling. In contrast, as the TM of human NKG2D is not permissive for association with DAP12 it requires no such regulatory region in the cytoplasmic domain and hence this structural feature has not been conserved.

NKG2D TM domains are necessary and sufficient to confer adapter specificity

As the mouse NKG2D truncation (mΔNKG2D) and mTM hEC chimeric NKG2D proteins paired with DAP12, it was possible that the EC portions of human or mouse NKG2D could be necessary for association with DAP12. To address this question and further to ask whether the TM regions of mouse and human NKG2D are sufficient to confer adapter specificity, we created chimeric proteins consisting of the TM domain of either mouse or human NKG2D fused to the EC domain of human CD69 (Fig. 6*a*). CD69 has some structural similarity to NKG2D, as it is also a type II TM-anchored homodimer with an EC region consisting of a single C type-like lectin domain (32–34). However, in contrast to NKG2D, CD69 does not pair with signaling adapters, such as DAP10 or DAP12, and does not possess charged amino acids in its TM region. A truncated form of CD69 consisting of only the TM and EC domains was also constructed as a control (in our study designated as ΔCD69) (Fig. 6*a*).

We tested the CD69 chimeras in the DAP10 or DAP12 reporter cells, as previously described, and found that the TM domain of NKG2D was necessary and sufficient to convey adapter specificity to the chimeric proteins (Fig. 6*b*). Although the control protein ΔCD69 did not pair with either adapter, the human TM NKG2D-CD69 protein was able to pair with DAP10, but not DAP12. In contrast, the mouse TM NKG2D-CD69 chimeric protein was able to associate equivalently with both DAP10 and DAP12.

We further wished to define requirements for DAP12 association. Closer examination of the mouse TM region revealed a second basic residue present in the mouse but not human TM region. We tested whether this second arginine residue (Fig. 2*a*, boxed)

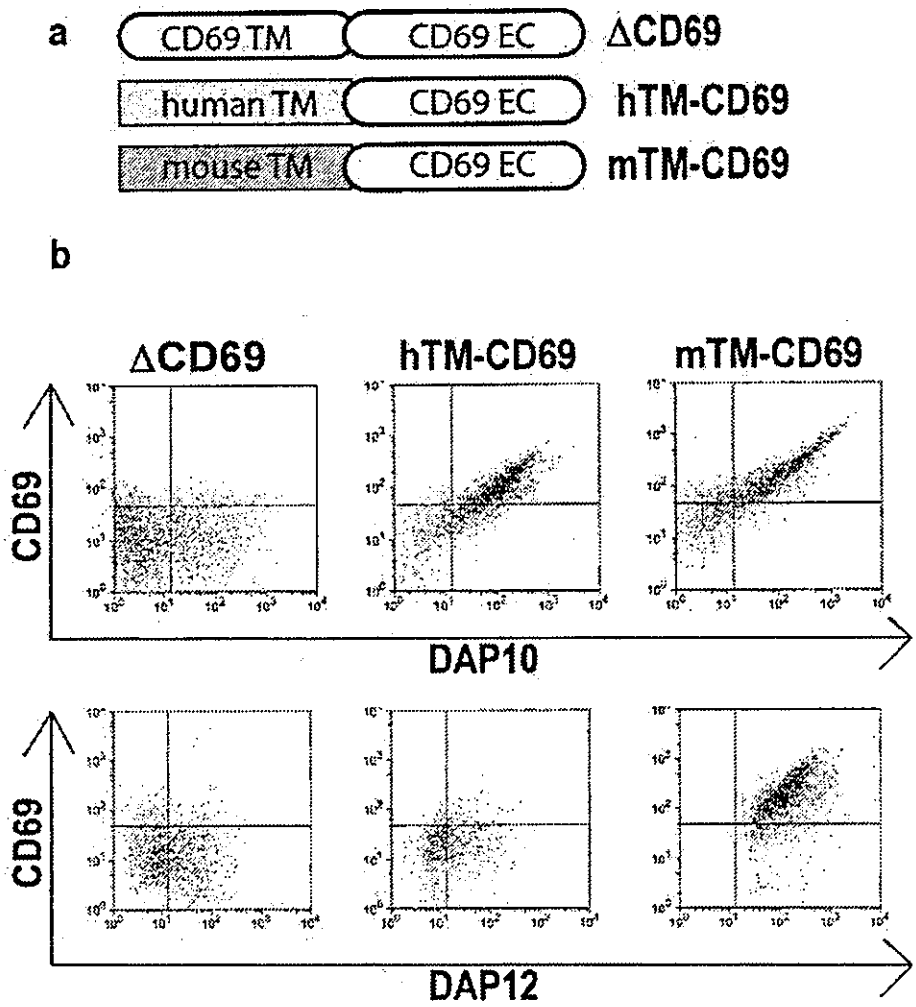

FIGURE 6. NKG2D TM regions are necessary and sufficient to confer DAP10 and DAP12 specificity. *a*, Schematic representation is shown of chimeric receptors containing the EC domain of human CD69 and the TM region of human or mouse NKG2D (as described in *Materials and Methods*). *b*, Ba/F3 reporter cells stably expressing Myc-DAP10 or Flag-DAP12 were infected with retroviruses with the indicated NKG2D TM-CD69 EC constructs in a vector containing an IRES-GFP element. Samples were stained with anti-human CD69 mAb and anti-epitope tag mAbs and analyzed by flow cytometry. Results shown are representative of at least three independent experiments.

was necessary for DAP12 association by mutating it to an alanine residue via site-directed mutagenesis. We found that an R→A mouse TM CD69 mutant still paired with DAP12, indicating that this putative second TM basic residue does not contribute to DAP12 association (data not shown).

These results formally demonstrate that the adapter specificity for human and mouse NKG2D lies exclusively in the TM domain, and this domain is necessary and sufficient to allow adapter pairing. A similar phenomenon has been observed for the receptor specificity of the human DAP10 and DAP12 signaling adapters. Chimeras between DAP10 and DAP12 have illustrated that the receptor specificity of these two adaptors also lies in their TM domains (27). Thus, for NKG2D, DAP10, and DAP12 all of the critical and necessary pairing interactions occur within the TM regions.

Overall, there is little conservation of the TM sequence of human and mouse NKG2D. Only a few amino acids have been conserved, conspicuously the arginine residue in the center of the TM. This extensive diversity in the sequence of the mouse and human NKG2D TM region precludes easy predictions about the critical residues in mouse NKG2D that permit or in human NKG2D prevent association with DAP12.

Discussion

Our results indicate a fundamental structural difference between mouse and human NKG2D. Although mouse NKG2D is capable of associating with both DAP10 and DAP12 signaling adapters, human NKG2D is only able to partner with DAP10. We show that this species difference can be mapped to the TM regions of mouse and human NKG2D. As DAP10 signals through a p85 phosphatidylinositol-3 kinase-mediated AKT pathway (16, 17), and as DAP12 signals through a Syk/ZAP70-mediated ITAM pathway (19), the ability of NKG2D to pair with various combinations of adapters represents its ability to initiate discreet signaling effects in mice, but not humans. Moreover, direct examination of NKG2D-dependent NK cell activation in DAP12-deficient humans suffering from the Nasu-Hakola disorder demonstrated that the NKG2D receptor functions normally with respect to its ability to induce cytolytic activity in the complete absence of DAP12.

Our findings are consistent with the studies of Billadeau et al. (21), which demonstrate that a chimeric protein with the cytoplasmic domain of human DAP10 was capable of triggering NK cell-mediated cytotoxicity. However, in these experiments the chimeric DAP10 was introduced into human NK cells expressing a functional DAP12 protein, leaving open the possibility of indirect interactions between the cytoplasmic domains of the chimeric DAP10 and endogenous DAP12 proteins. Our findings provide conclusive evidence for a DAP12-independent role of DAP10 in human NK cell NKG2D-mediated cytotoxicity.

Activated mouse NK cells expressing mNKG2D-S can thus signal through DAP10 and DAP12, whereas resting mouse NK cells and all human NK cells express long NKG2D and only signal

through DAP10. In many cases, DAP10 alone suffices to initiate cytotoxicity. This is evident from the fact that human NKG2D, which only uses DAP10, stimulates cytotoxicity independent of Syk kinases (21), as well as the evidence that NKG2D triggers cytotoxicity in mouse NK cells lacking DAP12 or Syk family kinases (20). In mice, DAP12 is also independently capable of initiating cytotoxicity through NKG2D-S, as demonstrated by experiments in DAP10-deficient mice (30). Furthermore, mouse NKG2D-S initiated DAP12 signaling contributes to proliferative responses and IFN-γ production (12). A role for DAP10 in IFN-γ production has been suggested using human NK cells and recombinant human NKG2D ligands (17, 31, 35).

It is not completely surprising that the mouse NKG2D TM region can associate with both DAP10 and DAP12 as these two adaptor proteins share significant homology. DAP10 and DAP12 share 20% sequence homology (16) and moreover their TM domains are very homologous in both sequence (45% homology) and structure (27). In the genomes of both mice and humans, the *DAP10* and *DAP12* genes are adjacent to one another, but in opposite transcriptional orientation (36), a circumstance that likely arose through gene duplication.

Our results illustrate that the TM domain of the immunoreceptor NKG2D provides signaling adapter specificity and accounts for the species difference. Although the human NKG2D TM associates only with DAP10, the mouse NKG2D TM associates with both DAP10 and DAP12. A comparison of NKG2D TM domain sequences across species demonstrates a close relationship between mouse and rat TM sequences (Fig. 2*c*). Furthermore, the only reported sequence of rat NKG2D lacks an N-terminal "tail" region and is thus structurally similar to mNKG2D-S. Based on the sequence similarity of mouse and rat TM regions and the absence on a potentially inhibitory tail sequence in rat NKG2D that could block DAP12 association, rat NKG2D likely pairs with DAP12. In contrast, other species such as macaque, cow, and pig, display TM sequences more homologous to human NKG2D and may solely signal through the DAP10 adapter protein, although this requires experimental verification.

Although many genes are highly conserved in sequence, expression and function between mice and humans, *NKG2D* represents a gene that has undergone evolutionary divergence between the two species. Although it acts as an innate immune receptor in both mice and humans, NKG2D demonstrates distinct signaling mechanisms in the two species and none of the human and mouse NKG2D ligands are highly conserved in primary sequence. For example, mice do not possess structural homologues of the human *MICA* and *MICB* genes that are present in the human MHC (37). Furthermore, although the human ULBP genes clearly are functional orthologs of the mouse *RAE-1*, *H60* and *MULT-1* genes they have diverged significantly and only demonstrate 15–20% sequence similarity (14). Expression of NKG2D also differs in humans and mice. Whereas all human $CD8^+$ T cells constitutively express NKG2D (4, 5), in mice only activated $CD8^+$ T cells possess NKG2D. Nonetheless, there is evidence that NKG2D is important in immune defense in mice and humans. Viruses and tumors have evolved immune evasion mechanisms to counter the effects of NKG2D (38–41). Thus, perhaps an evolutionary pressure from the host to fight rapidly evolving viral infections and tumors helps explain some of the divergence and distinctions of NKG2D between mice and humans.

Acknowledgments

We thank Drs. Naonobu Hutamura, Hidenori Matsuo, and Youichi Takahashi for their kind arrangements for collection of the blood samples. We also thank Dr. Kaori Sakuishi for flow cytometric analysis of the patients with Nasu-Hakola.

References

1. Lanier, L. L. 2001. On guard: activating NK cell receptors. *Nat. Immun. 2:23.*
2. Long, E. O. 1999. Regulation of immune responses through inhibitory receptors. *Annu. Rev. Immunol. 17:875.*
3. Houchins, J. P., T. Yabe, C. McSherry, and F. H. Bach. 1991. DNA sequence analysis of NKG2, a family of related cDNA clones encoding type II integral membrane proteins on human natural killer cells. *J. Exp. Med. 173:1017.*
4. Groh, V., A. Steinle, S. Bauer, and T. Spies. 1998. Recognition of stress-induced MHC molecules by intestinal epithelial $\gamma\delta$ T cells. *Science 279:1737.*
5. Bauer, S., V. Groh, J. Wu, A. Steinle, J. H. Phillips, L. L. Lanier, and T. Spies 1999. Activation of natural killer cells and T cells by NKG2D, a receptor for stress-inducible MICA. *Science 285:727.*
6. Cosman, D., J. Mullberg, C. L. Sutherland, W. Chin, R. Armitage, W. Fanslow, M. Kubin, and N. J. Chalupny. 2001. ULBPs, novel MHC class I-related molecules, bind to CMV glycoprotein UL16 and stimulate NK cytotoxicity through the NKG2D receptor. *Immunity 14:123.*
7. Diefenbach, A., A. M. Jamieson, S. D. Liu, N. Shastri, and D. H. Raulet. 2000. Ligands for the murine NKG2D receptor: expression by tumor cells and activation of NK cells and macrophages. *Nat. Immun. 1:119.*
8. Cerwenka, A., A. B. Bakker, T. McClanahan, J. Wagner, J. Wu, J. H. Phillips, and L. L. Lanier. 2000. Retinoic acid early inducible genes define a ligand family for the activating NKG2D receptor in mice. *Immunity 12:721.*
9. Bakker, A. B., J. Wu, J. H. Phillips, and L. L. Lanier. 2000. NK cell activation: distinct stimulatory pathways counterbalancing inhibitory signals. *Hum. Immunol. 61:18.*
10. Carayannopoulos, L. N., O. V. Naidenko, D. H. Fremont, and W. M. Yokoyama. 2002. Cutting edge: murine UL16-binding protein-like transcript 1: A newly described transcript encoding a high-affinity ligand for murine NKG2D. *J. Immunol. 169:4079.*
11. Cerwenka, A., and L. L. Lanier. 2001. Ligands for natural killer cell receptors: redundancy or specificity. *Immunol. Rev. 181:158.*
12. Diefenbach, A., E. Tomasello, M. Lucas, A. M. Jamieson, J. K. Hsia, E. Vivier, and D. H. Raulet. 2002. Selective associations with signaling proteins determine stimulatory versus costimulatory activity of NKG2D. *Nat. Immunol. 3:1142.*
13. Groh, V., R. Rhinehart, J. Randolph-Habecker, M. S. Topp, S. R. Riddell, and T. Spies. 2001. Costimulation of $CD8\alpha\beta$ T cells by NKG2D via engagement by MIC induced on virus-infected cells. *Nat. Immunol. 2:255.*
14. Cerwenka, A., and L. L. Lanier. 2001. Natural killer cells, viruses and cancer. *Nat. Rev. Immunol. 1:41.*
15. Raulet, D. H. 2003. Roles of the NKG2D immunoreceptor and its ligands. *Nat. Rev. Immunol. 3:781.*
16. Wu, J., Y. Song, A. B. H. Bakker, S. Bauer, V. Groh, T. Spies, L. L. Lanier, and J. H. Phillips. 1999. An activating receptor complex on natural killer and T cells formed by NKG2D and DAP10. *Science 285:730.*
17. Sutherland, C. L., N. J. Chalupny, K. Schooley, T. VandenBos, M. Kubin, and D. Cosman. 2002. UL16-binding proteins, novel MHC class I-related proteins, bind to NKG2D and activate multiple signaling pathways in primary NK cells. *J. Immunol. 168:671.*
18. Chang, C., J. Dietrich, A. G. Harpur, J. A. Lindquist, A. Haude, Y. W. Loke, A. King, M. Colonna, J. Trowsdale, and M. J. Wilson. 1999. Cutting edge: KAP10, a novel transmembrane adapter protein genetically linked to DAP12 but with unique signaling properties. *J. Immunol. 163:4651.*
19. Lanier, L. L., B. C. Corliss, J. Wu, C. Leong, and J. H. Phillips. 1998. Immunoreceptor DAP12 bearing a tyrosine-based activation motif is involved in activating NK cells. *Nature 391:703.*
20. Zompi, S., J. A. Hamerman, K. Ogasawara, E. Schweighoffer, V. L. Tybulewicz, J. P. Santo, L. L. Lanier, and F. Colucci. 2003. NKG2D triggers cytotoxicity in mouse NK cells lacking DAP12 or Syk family kinases. *Nat. Immunol. 4:565.*
21. Billadeau, D. D., J. L. Upshaw, R. A. Schoon, C. J. Dick, and P. J. Leibson 2003. NKG2D-DAP10 triggers human NK cell-mediated killing via a Syk-independent regulatory pathway. *Nat. Immunol. 4:557.*
22. Kondo, T., K. Takahashi, N. Kohara, Y. Takahashi, S. Hayashi, H. Takahashi, H. Matsuo, M. Yamazaki, K. Inoue, K. Miyamoto, and T. Yamamura. 2002. Heterogeneity of presenile dementia with bone cysts (Nasu-Hakola disease): three genetic forms. *Neurology 59:1105.*
23. Paloneva, J., M. Kestila, J. Wu, A. Salminen, T. Bohling, V. Ruotsalainen, P. Hakola, A. B. Bakker, J. H. Phillips, P. Pekkarinen, et al. 2000. Loss-of-function mutations in TYROBP (DAP12) result in a presenile dementia with bone cysts. *Nat Genet. 25:357.*
24. Lanier, L. L., J. J. Ruitenberg, and J. H. Phillips. 1988. Functional and biochemical analysis of CD16 antigen on natural killer cells and granulocytes. *J. Immunol. 141:3478.*
25. Onuhsi, M., S. Kinoshita, Y. Morikawa, A. Shibuya, J. Phillips, L. L. Lanier, D. M. Gorman, G. P. Nolan, A. Miyajima, and T. Kitamura. 1996. Applications of retrovirus-mediated expression cloning. *Exp. Hematol. 24:324.*
26. Kinsella, T. M., and G. P. Nolan. 1996. Episomal vectors rapidly and stably produce high-titer recombinant retrovirus. *Hum. Gene Ther. 7:1405.*
27. Wu, J., H. Cherwinski, T. Spies, J. H. Phillips, and L. L. Lanier. 2000. DAP10 and DAP12 form distinct, but functionally cooperative, receptor complexes in natural killer cells. *J. Exp. Med. 192:1059.*
28. Bakker, A. B., E. Baker, G. R. Sutherland, J. H. Phillips, and L. L. Lanier. 1999. Myeloid DAP12-associating lectin (MDL)-1 is a cell surface receptor involved in the activation of myeloid cells. *Proc. Natl. Acad. Sci. USA 96:9792.*
29. Lanier, L. L. 2003. Natural killer cell receptor signaling. *Curr. Opin. Immunol. 15:308.*

30. Gilfillan, S., E. L. Ho, M. Cella, W. M. Yokoyama, and M. Colonna. 2002. NKG2D recruits two distinct adapters to trigger NK cell activation and costimulation. *Nat. Immunol. 3:1150.*
31. Andre, P., R. Castriconi, M. Espeli, N. Anfossi, T. Juarez, S. Hue, H. Conway, F. Romagne, A. Dondero, M. Nanni, et al. 2004. Comparative analysis of human NK cell activation induced by NKG2D and natural cytotoxicity receptors. *Eur. J. Immunol. 34:961.*
32. Hamann, J., H. Fiebig, and M. Strauss. 1993. Expression cloning of the early activation antigen CD69, a type II integral membrane protein with a C-type lectin domain. *J. Immunol. 150:4920.*
33. Lopez-Cabrera, M., A. G. Santis, E. Fernandez-Ruiz, R. Blacher, F. Esch, P. Sanchez-Mateos, and F. Sanchez-Madrid. 1993. Molecular cloning, expression, and chromosomal localization of the human earliest lymphocyte activation antigen AIM/CD69, a new member of the C-type animal lectin superfamily of signal-transmitting receptors. *J. Exp. Med. 178:537.*
34. Ziegler, S. F., F. Ramsdell, K. A. Hjerrild, R. J. Armitage, K. H. Grabstein, K. B. Hennen, T. Farrah, W. C. Fanslow, E. M. Shevach, and M. R. Alderson. 1993. Molecular characterization of the early activation antigen CD69: a type II membrane glycoprotein related to a family of natural killer cell activation antigens. *Eur. J. Immunol. 23:1643.*
35. Kubin, M., L. Cassiano, J. Chalupny, W. Chin, D. Cosman, W. Fanslow, J. Mullberg, A.-M. Rousseau, D. Ulrich, and R. Armitage. 2001. ULBP1, 2, 3: novel MHC class I-related molecules that bind to human cytomegalovirus glycoprotein UL16, activate NK cells. *Eur. J. Immunol. 31:1428.*
36. Wilson, M. J., A. Hamle, and J. Trowsdale. 2001. The mouse Dap10 gene. *Immunogenetics 53:347.*
37. Bahram, S., M. Bresnahan, D. E. Geraghty, and T. Spies. 1994. A second lineage of mammalian major histocompatibility complex class I genes. *Proc. Natl. Acad. Sci. USA 91:6259.*
38. Rolle, A., M. Mousavi-Jazi, M. Eriksson, J. Odeberg, C. Soderberg-Naucler, D. Cosman, K. Karre, and C. Cerboni. 2003. Effects of human cytomegalovirus infection on ligands for the activating NKG2D receptor of NK cells: up-regulation of UL16-binding protein (ULBP)1 and ULBP2 is counteracted by the viral UL16 protein. *J. Immunol. 171:902.*
39. Lodoen, M., K. Ogasawara, J. A. Hamerman, H. Arase, J. P. Houchins, E. S. Mocarski, and L. L. Lanier. 2003. NKG2D-mediated natural killer cell protection against cytomegalovirus is impaired by viral gp40 modulation of retinoic acid early inducible 1 gene molecules. *J. Exp. Med. 197:1245.*
40. Groh, V., J. Wu, C. Yee, and T. Spies. 2002. Tumour-derived soluble MIC ligands impair expression of NKG2D and T-cell activation. *Nature 419:734.*
41. Wu, J., N. J. Chalupny, T. J. Manley, S. R. Riddell, D. Cosman, and T. Spies. 2003. Intracellular retention of the MHC class I-related chain B ligand of NKG2D by the human cytomegalovirus UL16 glycoprotein. *J. Immunol. 170:4196.*

DOI: 10.1093/brain/awh219 *Brain* (2004), **127**, 1917–1927

The regulatory role of natural killer cells in multiple sclerosis

Kazuya Takahashi,[1] Toshimasa Aranami,[1] Masumi Endoh,[1,2] Sachiko Miyake[1] and Takashi Yamamura[1]

[1]*Department of Immunology, National Institute of Neuroscience, National Center of Neurology and Psychiatry, 4-1-1 Ogawahigashi, Kodaira, Tokyo 187-8502 and* [2]*Department of Bioregulation, Leprosy Research Center, National Institute of Infectious Diseases, 4-2-1 Aoba, Higashimurayama, Tokyo 189-0002, Japan*

Correspondence to: Takashi Yamamura, Department of Immunology, National Institute of Neuroscience, National Center of Neurology and Psychiatry, 4-1-1 Ogawahigashi, Kodaira, Tokyo 187-8502, Japan
E-mail: yamamura@ncnp.go.jp

Summary

Multiple sclerosis is a chronic demyelinating disease of presumed autoimmune pathogenesis. The patients with multiple sclerosis typically shows alternating relapse and remission in the early stage of illness. We previously found that in the majority of multiple sclerosis patients in a state of remission, natural killer (NK) cells contain unusually high frequencies of the cells expressing CD95 (Fas) on their surface (>36.0%). Here we report that in such 'CD95$^+$ NK-high' patients, NK cells may actively suppress potentially pathogenic autoimmune T cells that can mediate the inflammatory responses in the CNS. Using peripheral blood mononuclear cells (PBMCs) derived from 'CD95$^+$ NK-high' or 'CD95$^+$ NK-low' multiple sclerosis in a state of remission, we studied the effect of NK cell depletion on the memory T cell response to myelin basic protein (MBP), a major target antigen of multiple sclerosis. When we stimulated PBMCs of the 'CD95$^+$ NK-high' multiple sclerosis after depleting CD56$^+$ NK cells, a significant proportion of CD4$^+$ T cells (1/2000 to 1/200) responded rapidly to MBP by secreting interferon (IFN)-γ, whereas such a rapid T cell response to MBP could not be detected in the presence of NK cells. Nor did we detect the memory response to MBP in the 'CD95$^+$ NK-low' multiple sclerosis patients in remission or healthy subjects, regardless of whether NK cells were depleted or not. Depletion of cells expressing CD16, another NK cell marker, also caused IFN-γ secretion from MBP-reactive CD4$^+$ T cells in the PBMCs from 'CD95$^+$ NK-high' multiple sclerosis. Moreover, we showed that NK cells from 'CD95$^+$ NK-high' multiple sclerosis could inhibit the antigen-driven secretion of IFN-γ by autologous MBP-specific T cell clones *in vitro*. These results indicate that NK cells may regulate activation of autoimmune memory T cells in an antigen non-specific fashion to maintain the clinical remission in 'CD95$^+$ NK-high' multiple sclerosis patients.

Keywords: multiple sclerosis; myelin basic protein; NK cell; NK2; T cell–NK cell interaction

Abbreviations: CBA = cytokine bead array; HLA = human leukocyte antigen; IFN = interferon; IL = interleukin; MBP = myelin basic protein; MS-rel = multiple sclerosis in relapse; MS-rem = multiple sclerosis in remission; NK = natural killer; NK2 = NK type 2; OVA = ovalbumin; PBMCs = peripheral blood mononuclear cells; PI = propidium iodide; PLP = proteolipid protein; TCC = T-cell clone; TNF = tumour necrosis factor

Received January 14, 2004. Revised March 18, 2004. Second revision April 10, 2004. Accepted April , 2004. Advanced Access publication June 30, 2004

Introduction

Multiple sclerosis is a chronic neurological disease the pathology of which is characterized by multiple foci of inflammatory demyelinating lesions accompanying a variable degree of axonal changes (Bjartmar and Trapp, 2001). Regarding the pathogenesis of multiple sclerosis, studies have indicated that autoimmune T cells targeting myelin components play a crucial role in mediating the inflammatory process, particularly in the early stages of relapsing–remitting multiple sclerosis (Steinman, 2001). A number of laboratories have studied the properties of potentially pathogenic autoimmune T cell clones (TCC) reactive to myelin antigens such as myelin basic protein (MBP) and proteolipid protein (PLP), which have been derived from the peripheral blood of multiple sclerosis (Ota *et al.*, 1990; Pette *et al.*, 1990; Martin *et al.*, 1991; Ohashi *et al.*, 1995). The large majority of the TCC are CD4$^+$ and produce T helper type 1 (Th1) cytokines

such as interferon (IFN)-γ after recognizing the myelin peptide bound to human leukocyte antigen (HLA)-DR molecules. These results are consistent with the idea that the inflammatory process of multiple sclerosis is triggered by invasion of autoimmune Th1 cells into the CNS, and that exogenous or endogenous factors altering the Th1/Th2 balance may influence the disease activity. The relevance of this postulate is actually supported by clinical observations that Th2-inducing medications, such as copolymer-1, are beneficial for multiple sclerosis (Duda *et al.*, 2000; Neuhaus *et al.*, 2000), and that administration of IFN-γ showed deleterious effects on multiple sclerosis in previous clinical trials (Panitch *et al.*, 1987).

Although there are a number of candidate target antigens for multiple sclerosis, MBP is thought to be a primary target for autoimmune T cells, at least in some patients (Bielekova *et al.*, 2000). It is of note that MBP- or PLP-specific TCC can be established not only from multiple sclerosis, but also from peripheral blood of healthy subjects, which raised the intriguing issue as to how healthy subjects are protected from self-attack by the potentially pathogenic autoimmune Th1 cells. Although much remains to be clarified, studies in the last decade have showed that regulatory cells are involved in prevention of or recovery from autoimmune diseases in rodent (Das *et al.*, 1997; Zhang *et al.*, 1997; Olivares-Villagomez *et al.*, 1998; Sakaguchi *et al.*, 2001). This allows us to speculate that regulatory cells may contribute to protecting healthy subjects from developing autoimmune diseases such as multiple sclerosis, or to prohibiting acute attacks or enhancing the recovery from clinical exacerbations in patients with relapsing–remitting multiple sclerosis.

Whereas regulatory cells constitute various lymphoid populations, substantial evidence supports that natural killer (NK) cells play significant roles in protecting against autoimmune diseases (Zhang *et al.*, 1997; Matsumoto *et al.*, 1998; Smeltz *et al.*, 1999). In fact, it has previously been demonstrated that NK cell depletion augments the severity of a model for multiple sclerosis, experimental autoimmune encephalomyelitis (EAE) (Zhang *et al.*, 1997; Matsumoto *et al.*, 1998), which can be induced by sensitization against CNS myelin component. Given that autoimmune Th1 cells would mediate the pathology of EAE, we propose a possible involvement of NK cells in suppressing autoimmune Th1 cells in multiple sclerosis.

With the hypothesis that NK cells may contribute to maintaining the remission in relapsing–remitting multiple sclerosis, we have previously examined the cytokine production and surface phenotype of NK cells freshly isolated from the peripheral blood mononuclear cells (PBMCs) of multiple sclerosis in remission (MS-rem) or relapse (MS-rel) (Takahashi *et al.*, 2001). The results demonstrate that NK cells in MS-rem (but not MS-rel) are characterized by a remarkable elevation of interleukin (IL)-5 mRNA and a decreased expression of IL-12Rβ2 mRNA, as well as a higher percentage of $CD95^+$ cells among the $CD56^+$ NK cells. These features of the cells are reminiscent of NK type 2 (NK2) cells, which can be induced *in vitro* in the presence of IL-4 and of anti-IL-12 antibodies (Peritt *et al.*, 1998). The NK2 cells induced from PBMCs of healthy subjects inhibit the generation of IFN-γ-secreting Th1 cells from the PBMCs of the same subjects (Takahashi *et al.*, 2001), leading us to postulate that NK2-like cells detected in MS-rem may play a regulatory role. While the NK2-like features were found to be lost in patients at acute relapsing state, they tended to be restored along with clinical recovery. Obviously, these results do not imply that clinically diagnosed MS-rem represents a homogeneous condition. In fact, the parameters characteristic for NK2-like cells (i.e. up-regulation of IL-5 mRNA and an increased frequency of $CD95^+$ cells) showed a substantial variance in MS-rem, indicating their heterogeneity.

More recently, we have noticed that MS-rem can be divided into two subgroups, '$CD95^+$ NK-high' and '$CD95^+$ NK-low', according to the frequency of $CD95^+$ cells among NK cells. Here, we demonstrate that these two groups significantly differ in the responsiveness to MBP *ex vivo* in an NK-cell-depleted condition. Namely, NK-deleted PBMCs from '$CD95^+$ NK-high' multiple sclerosis responded rapidly to MBP, as assessed by the frequency of IFN-γ-secreting $CD4^+$ T cells at 8 h after stimulation with MBP, whereas those from the '$CD95^+$ NK-low' or from healthy subjects responded only marginally. Moreover, we showed that NK cells from a '$CD95^+$ NK-high' multiple sclerosis could inhibit the antigen-driven secretion of IFN-γ by MBP-specific TCC established from the same patient. These results demonstrate, for the first time to our knowledge, that NK cell depletion leads to augmentation of memory T cell response to an autoantigen in human, and that an elaborate interplay between NK cells and MBP-specific memory T cells may be involved in the regulation of multiple sclerosis in '$CD95^+$ NK-high' patients.

Material and methods

Subjects

To clarify the heterogeneity among patients with MS-rem regarding NK cell phenotype, we first examined 30 patients with MS-rem (male/female = 11/19; aged 37.7 ± 11.1 years) for the lymphoid cell expression of CD95. As a control for multiple sclerosis, we examined 26 healthy sex- and age-matched subjects (male/female = 11/15; aged 39.9 ± 12.2 years). Furthermore, for a new cohort of 14 patients with MS-rem (male/female = four/10; aged 39.2 ± 10.7 years) (Table 1) and 14 healthy subjects (male/female = five/nine; aged 35.3 ± 8.0 years), we conducted the cytokine secretion assay as well as flow cytometer analysis for the frequency of $CD95^+$ NK cells. Two of the patients were examined again after a 1-year interval.

Written informed consent was obtained from all patients and healthy volunteers and the study was approved by the Ethics Committee of the National Center of Neuroscience (NCNP). All patients fulfilled standard criteria for the diagnosis of relapsing–remitting multiple sclerosis (Poser *et al.*, 1983; McDonald *et al.*, 2001). The clinical status of multiple sclerosis (MS-rem or MS-rel) was operationally determined as described previously (Takahashi *et al.*, 2001). In brief, we selected MS-rem patients for study who had been clinically stable without any immunosuppressive medications for >3 months, and had shown no sign of new lesions as assessed by a recent MRI scan with gadolinium enhancement. None of our patients represented the pure optic-spinal form of multiple sclerosis (Misu *et al.*, 2002), which may be rather unique to Japanese populations.

Table 1 *List of the PBMC samples examined for the frequency of memory Th1 cells*

Information on patients			
PBMC code	Age (years)/sex	$CD95^+$ NK frequency	EDSS#
#1	43/M	High	2.5
#2	30/F	High	2.5
#3	53/M	High	1.0
#4	39/F	High	3.5
#5	28/F	High	1.0
#6*	35/M	Low	2.0
#7**	57/F	Low	3.0
#8	31/M	Low	1.0
#9	29/F	Low	3.0
#10	38/F	Low	2.0
#11	59/F	High	3.5
#12*	36/M	High	2.0
#13**	58/F	High	3.0
#14	33/F	High	6.5
#15	29/F	Low	1.0
#16	45/F	Low	4.0

The samples marked with * or ** are derived from the same patients, with an interval of 1 year between samples. The phenotype of both of these patients changed from '$CD95^+$ NK-low' to '$CD95^+$ NK-high'. M = male; F = female; EDSS = Expanded Disability Status Scale.

Reagents

Anti-CD3-FITC or -ECD, anti-CD4-PC5, anti-CD8-FITC, anti-CD16-Phytoerythrin, and anti-CD56-PC5 or -PE mAbs were purchased from IMMUNOTECH (Marseille, France). Anti-CD57-FITC, anti-CD69-PE, anti-CD94-FITC, anti-CD95-FITC, -Cych or -PE, anti-CD158a-FITC, anti-NKB1-FITC, and anti-HLA-DR-FITC mAbs were purchased from BD PharMingen (San Jose, CA, USA). Human MBP was purified with a modification of previously described methods (Deibler *et al.*, 1972, 1995).

Cell preparation and NK cell deletion

Shortly after drawing peripheral blood, PBMCs were separated by density gradient centrifugation with Ficoll-Hypaque™ PLUS (Amersham Biosciences, Uppsala, Sweden). They were washed three times in phosphate-buffered saline (PBS), and resuspended at 1×10^6 cells/ml in AIM-V culture medium (Invitrogen Corp., Carlsbad, CA, USA) containing 2 mM L-glutamine, 100 U/ml penicillin and 100 μg/ml streptomycin (Life Technologies, Rockville, MD, USA). NK cells were depleted from the PBMCs with either CD56- or CD16-MicroBeads (Miltenyi Biotech, Gradbach, Germany), following the protocol provided by the manufacturer.

T cell clones

$CD4^+$ TCC were generated from a '$CD95^+$ NK-high' multiple sclerosis patient (HLA-DRB1*1502) by repeated selection against human whole MBP with modification of a previously described method (Pette *et al.*, 1990). The TCC proliferated and secreted Th1 cytokines specifically in response to MBP, and the proliferative response and cytokine production was greatly reduced in the presence of antibodies against HLA-DR. The DR-restricted clone cells were grown in AIM-V medium supplemented with 2 mM L-glutamine, 100 U/ml penicillin and 100 μg/ml streptomycin.

T-cell stimulation with MBP

To assess the presence of memory MBP-reactive T cells in the peripheral blood, fresh PBMCs or NK-deleted PBMCs were stimulated for 8 h with 10 μg/ml MBP in 96-well round-bottomed plates at 2×10^5 cells/well, and then analysed for the presence of IFN-γ-secreting cells using the cytokine secretion assay. To evaluate the regulatory function of NK cells from '$CD95^+$ NK-high' multiple sclerosis, resting cells of MBP-specific TCC (2×10^4 cells/well) were stimulated with 10 μg/ml MBP in the presence of X-irradiated (5000 rad) autologous total PBMCs or $CD56^+$ NK-deleted PBMCs (1×10^5 cells/well) for 8 h prior to the cytokine secretion assay, and for 60 h to determine the proliferation of the TCC. To assess cell proliferation, we counted incorporation of [^{3}H]thymidine (1 μCi/well) during the final 12 h with a beta-1205 counter (Pharmacia, Uppsala, Sweden).

Cytokine secretion assay

We used a commercial kit from Miltenyi Biotech to identify T cells secreting IFN-γ. The principle of this assay has been described previously (Manz *et al.*, 1995). Briefly, cells were stained with IFN-γ capture antibody 8 h after stimulation with MBP or ovalbumin (OVA), then washed and cultured again for 45 min. They were stained with PE-conjugated IFN-γ detection antibody, together with anti-human CD3-FITC and -CD4-PC5, then washed and resuspended in PBS containing propidium iodide (PI) (BD PharMingen). Samples were analysed using flow cytometry.

Cytokine bead array

The levels of IL-2, -4, -5, -10, tumour necrosis factor (TNF)-α and IFN-γ in the culture supernatants were measured by cytokine bead array (CBA) (BD PharMingen), in which six bead populations with distinct fluorescence intensities are coated with capture antibodies specific for each cytokine (Cook *et al.*, 2001). The cytokine capture beads were mixed with the PE-conjugated detection antibodies and then incubated with recombinant standards or supernatant samples to form sandwich complexes. After washing the beads, sample data were acquired using the flow cytometer and were analysed with the BD CBA Analysis Software® (BD PharMingen).

Results

An increased frequency of $CD95^+$ NK cells distinguishes a subgroup of multiple sclerosis

As we have reported previously (Takahashi *et al.*, 2001), whereas proportions of $CD3^-$ $CD56^+$ NK cells in fresh PBMCs weakly express CD95 on their surface, the frequency of $CD95^+$ NK cells is significantly elevated in MS-rem as compared with healthy subjects or MS-rel. We have further noticed that MS-rem can be divided into two subgroups according to the frequency (%) of $CD95^+$ cells among NK cells (Fig. 1A; see also the left panels in Figs 1B and 2A, showing the distinction between $CD95^+$ and $CD95^-$ cells). When we determined the mean + 2 SD value for healthy subjects (35.86%) as an upper boundary for healthy subjects,

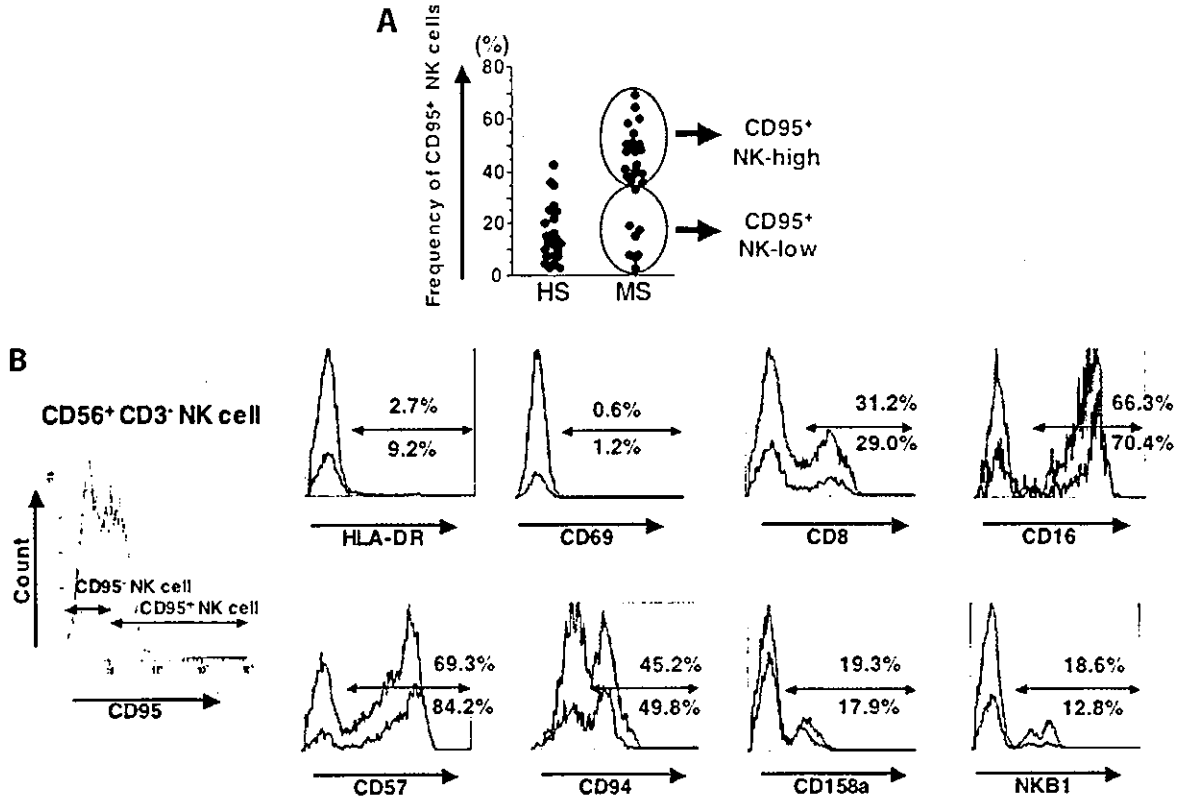

Fig. 1 Characterization of CD95$^+$ NK cells from 'CD95$^+$ NK-high' multiple sclerosis. (A) Multiple sclerosis patients in remission (MS-rem) can be subgrouped into 'CD95$^+$ NK-high' and 'CD95$^+$ NK-low'. Freshly isolated PBMCs from 26 healthy subjects or 30 MS-rem were stained with the combination of anti-CD3-FITC, -CD56-PC5 and -CD95-PE, and evaluated for the frequency of CD95$^+$ cells in the CD56$^+$CD3$^-$ NK cell population (the fluorescence intensity for CD95 expression is shown in the histograms in **B** and Fig. 2A). Note that flow fluorocytometric analysis was completed within 2 h after drawing blood in order to avoid spontaneous death of CD95$^+$ cells. (B) Comparison of CD95$^+$ versus CD95$^-$ NK cells in the expression of various surface molecules. We stained the PBMCs from 'CD95$^+$ NK-high' patients with the panel of antibodies for surface molecules expressed by NK cells. Red lines represent the histogram gated for CD95$^-$ NK cells and blue lines for CD95$^+$ NK cells. Values in red and in blue represent the positive percentage in CD95$^-$ and CD95$^+$ cells, respectively. As indicated, CD95$^+$ NK cells did not differ significantly from CD95$^-$ NK cells in the staining pattern for each antibody regarding the proportion of positive cells as well as the mean fluorescence intensity. Shown are the results of a representative case.

three-quarters of MS-rem had a percentage value higher than this boundary. We defined these patients in remission with a higher frequency of CD95$^+$ cells in NK cells as 'CD95$^+$ NK-high' multiple sclerosis, and the rest as 'CD95$^+$ NK-low' (Fig. 1A). In contrast to CD56$^+$ NK cells, CD3$^+$CD56$^-$ T cells and CD3$^+$CD56$^+$ NK T cells were not different between healthy subjects and multiple sclerosis patients as regards the frequency of CD95$^+$ cells (data not shown), which directed our attention to the analysis of CD56$^+$ NK cells.

Because NK cells from MS-rem were found to express a larger amount IL-5 mRNA, and since they were neither defective in cytolytic function nor reduced in number (Takahashi *et al.*, 2001), we hypothesized that the CD95 expression may reflect an activation state of the NK cells. To test this hypothesis, we compared the CD95$^+$ and CD95$^-$ NK populations derived from 'CD95$^+$ NK-high' patients by flow cytometry. Histogram plot analysis for the proportion of positive cells and for mean fluorescence intensity showed that the two populations are analogous in the expression of HLA-DR, CD69, CD8, CD16, CD57, CD94, CD158a and NKB1 (Fig. 1B). Whereas HLA-DR and CD69 molecules are regarded as cell activation markers, few populations of CD95$^+$ NK cells from multiple sclerosis or healthy subjects expressed these molecules. These results do not support the idea that the CD95$^+$ NK cells are in a state of activation, nor do they indicate that the CD95$^+$ cells represent a unique subset of monoclonal or oligoclonal origin. It has recently been suggested that CD56^{bright} NK cells may represent a distinct subset (Jacobs *et al.*, 2001). However, we saw no difference in the proportion of CD56^{bright} cells between CD95$^+$ and CD95$^-$ NK cells (data not shown).

CD56$^+$ NK cell depletion induces the rapid activation of MBP-reactive memory T cells in PBMCs from 'CD95$^+$ NK-high' multiple sclerosis

We have previously shown that the CD95$^+$ NK cells found in multiple sclerosis patients resemble the NK cells that can be induced in culture in the presence of IL-4 and anti-IL-12

mAb [referred to as 'NK2-like cells' according to the definition by Peritt *et al.* (1998)]. We also found that Peritt's NK2 cells induced *in vitro* inhibited the induction of IFN-γ-secreting T cells from peripheral T cells after stimulation with phorbol myristate acetate and ionomycin (Takahashi *et al.*, 2001). Based on these observations, we speculated that NK cells might prohibit Th1 cell activation in the remission of multiple sclerosis in an antigen-non-specific manner, and contribute to maintaining the remission. However, it remained an open question as to whether the NK2-like cells found in MS-rem would indeed regulate pathogenic autoimmune T cells *in vivo*. To investigate functions of NK cells in MS-rem, we evaluated the effect of NK cell depletion on the peripheral T cell response to MBP, a major target antigen of multiple sclerosis (Bielekova *et al.*, 2000). In brief, we depleted $CD56^+$ cells from the PBMCs with a magnetic sorter, and then stimulated the NK-deleted populations as well as whole PBMCs with MBP *in vitro* for 8–24 h. Subsequently, we detected the antigen-responsive T cells based on the secretion of IFN-γ (Manz *et al.*, 1995). The preparatory experiments revealed that 8 h of stimulation provides an optimal condition yielding a low background (0–0.03%). This novel assay enables us to selectively detect memory-type Th1 cells that can respond rapidly to antigen, whereas previous assays that depend on long-term cultures (Pette *et al.*, 1990; Martin *et al.*, 1992) evaluate not only memory but also naive T cells. Of note, there is a general consensus that peripheral blood of multiple sclerosis patients contains MBP-reactive T cells that are activated and/or differentiated into memory T cells (Allegretta *et al.*, 1990; Martin *et al.*, 1992; Zhang *et al.*, 1994; Lovett-Racke *et al.*, 1998; Scholz *et al.*, 1998).

We examined 16 PBMC samples from 14 MS-rem patients (nine samples from '$CD95^+$ NK-high', and seven from '$CD95^+$ NK-low') and 14 healthy subjects (see Table 1). When freshly isolated PBMCs were stimulated with MBP before NK cell depletion, four MS-rem and five healthy subjects samples showed a marginal response to MBP (0.01–0.03% increase of IFN-γ-positive cells among $CD4^+$ T cells). We did not find any significant response to MBP with the other PBMC samples. In contrast, when cells were stimulated with MBP after deleting $CD56^+$ NK cells, a significant response with a stimulatory index >3 was detected in seven of the nine '$CD95^+$ NK-high' samples, and a marginal response was detected in two (Fig. 2A and B). Of note, none of the NK-deleted samples from the '$CD95^+$ NK-low' patients and healthy subjects showed a definitive response to MBP. The difference for the '$CD95^+$ NK-high' versus the '$CD95^+$ NK-low' or healthy subjects was statistically significant (Fig. 2B). These *ex vivo* experiments have revealed that the '$CD95^+$ NK-high' patients may possess a higher number of T cells that can rapidly respond to MBP (MBP-specific memory T cells), compared with '$CD95^+$ NK-low' MS-rem or healthy subjects. In other words, they provide strong evidence for clonal expansion of memory autopathogenic T cells in the '$CD95^+$ NK-high' patients. However, as we could demonstrate an increase of the memory autoimmune T cells only after depleting NK cells, we interpreted that the potentially hazardous autoimmune T cells are being controlled by counter-regulatory NK cells in the '$CD95^+$ NK-high' patients. Of note, previous studies relying on alternative assays have revealed the presence of MBP-reactive T cells with activated and/or memory phenotypes at similar high frequencies in not all, but a major portion, of multiple sclerosis patients (Allegretta *et al.*, 1990; Zhang *et al.*, 1994; Bieganowska *et al.*, 1997; Lovett-Racke *et al.*, 1998; Scholz *et al.*, 1998; Illés *et al.*, 1999).

We conducted the same assay with a foreign antigen OVA in three of the '$CD95^+$ NK-high' (PBMC codes #3, #4 and #5 in Table 1) and one of the '$CD95^+$ NK-low' samples (#6). However, OVA-reactive T cells could not be detected in any sample of the fresh or NK-deleted PBMCs (data not shown). Because NK cells cannot discriminate T cells with different antigen specificities, the negative response to OVA in the four multiple sclerosis patients was interpreted to mean that they do not possess clonally expanded memory T cells reactive to OVA.

Depletion of $CD16^+$ NK cells also allows detection of MBP-reactive memory T cells in PBMCs from '$CD95^+$ NK-high' multiple sclerosis

Although we used anti-CD56 magnetic beads to deplete NK cells in the above experiments, the method would also deplete $CD3^+CD56^+$ NK T cells that may possibly play a role in the regulation of autoimmunity. To evaluate the possible contribution of $CD3^+CD56^+$ NK T cells, we next depleted NK cells from PBMCs from two '$CD95^+$ NK-high' patients on the basis of their expression of CD16. We found that after treatment with CD16-MicroBeads, almost all of $CD56^+$ NK cells are deleted, but $CD56^+CD3^+$ NKT cells remain largely untouched (Fig. 3A). However, like $CD56^+$-cell-deleted PBMCs, the $CD16^+$-cell-deleted PBMCs responded to MBP, as assessed by the induction of IFN-γ-secreting $CD4^+$ T cells (Fig. 3B). The responses found in the two patients were considered significant with regard to both percentage increase of IFN-γ-secreting cells (0.08% and 0.04%) and the stimulatory index (9.0 and 5.0) obtained after MBP stimulation. This result indicates that responsible cells to regulate autoimmune T cells in '$CD95^+$ NK-high' multiple sclerosis are not $CD56^+CD3^+$ NK T cells but NK cells.

Unfortunately, it remains unclear whether only $CD95^+$ NK cells play a regulatory role in '$CD95^+$ NK-high' multiple sclerosis or whether $CD95^-$ cells could also exhibit regulatory functions in the patients. We attempted to compare directly the function of $CD95^+$ and $CD95^-$ populations. However, isolation of $CD95^+$ NK cells with a cell sorter invariably induced cell activation as revealed by the expression of various activation markers. Furthermore, the isolated cells tended to die rapidly, probably due to CD95 ligation by the antibody (data not shown).

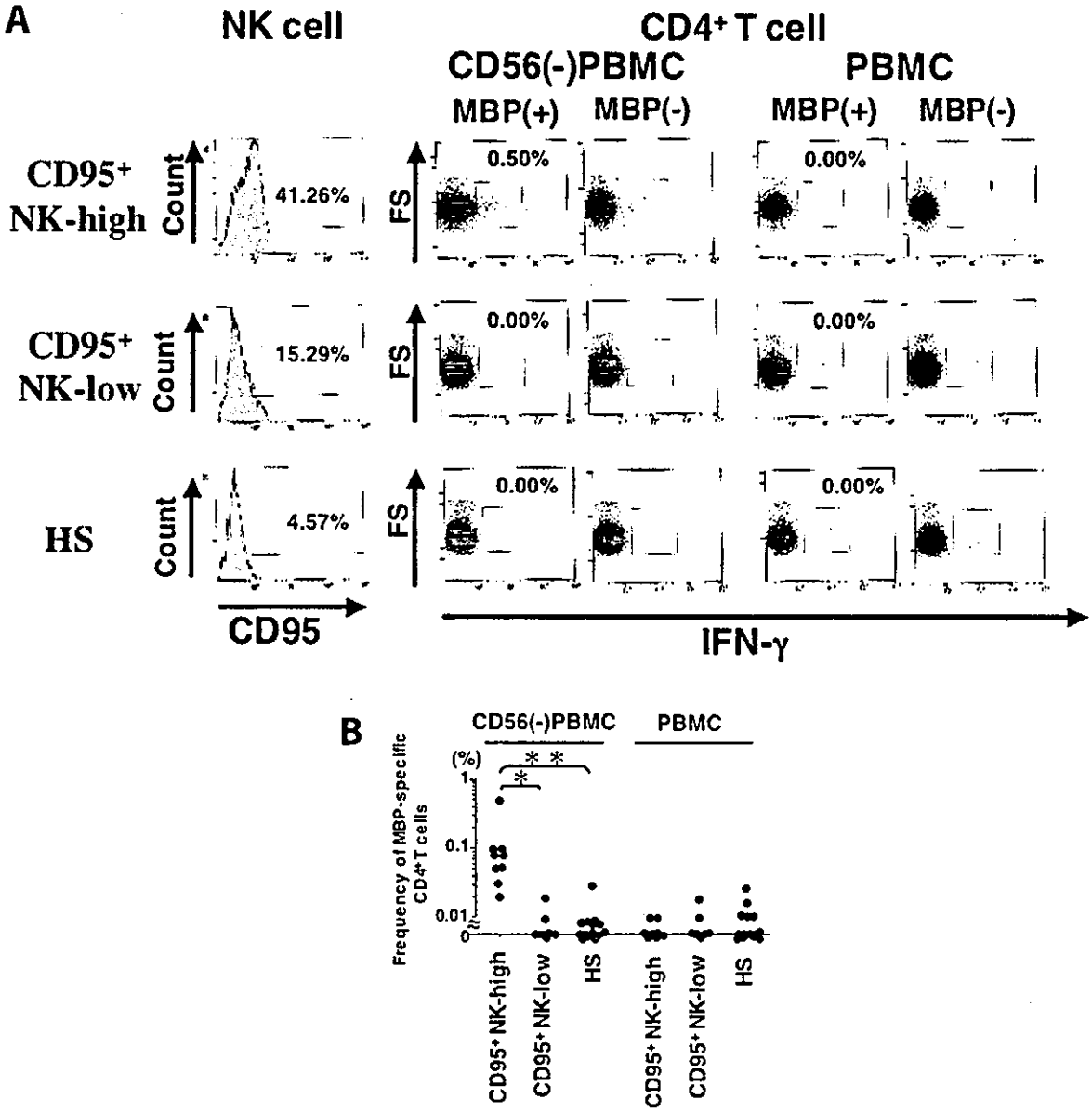

Fig. 2 Evidence for the role of NK cells in the regulation of MBP-reactive memory T cells in 'CD95$^+$ NK-high' multiple sclerosis. (**A**) IFN-γ secretion assay for NK-cell-deleted PBMCs and freshly isolated PBMCs. Whole PBMCs or PBMCs depleted for CD56$^+$ NK cells [CD56(−) PBMC] from the 'CD95$^+$ NK-high' multiple sclerosis (n = 9), 'CD95$^+$ NK-low' multiple sclerosis (n = 7) or healthy subjects (n = 14) were stimulated with 10 μg/ml of human MBP for 8 h for the IFN-γ secretion assay. The cells were also stained with anti-CD4-PC5 and -CD3-FITC, and the CD4$^+$CD3$^+$ and PI$^-$ cells were gated for analysis. Here we show representative results from 'CD95$^+$ NK-high' (*top*), 'CD95$^+$ NK-low' (*middle*) and healthy subjects (*bottom*). The IFN-γ-secreting CD4$^+$ T cells are shown as red dots; blue dots represent IFN-γ-negative cells. The histograms demonstrate the level of CD95 expression on the fresh CD56$^+$ NK cells from each individual, and the attached values show the frequency of CD95$^+$ cells. (**B**) Frequency (%) of MBP-reactive memory T cells among CD4$^+$ T cells. By using the cytokine secretion assay, we determined the frequency of IFN-γ-positive cells among CD4$^+$ T cells in each individual after culture with or without MBP. Here we plot the Δ% values [(%) with MBP − (%) without MBP], which represent the frequency of MBP-reactive CD4$^+$ T cells in each subject. Kruskal–Wallis test with Scheffe's F *post hoc* test was used for statistical analysis. $^*P < 0.05$; $^{**}P < 0.02$.

NK cells from 'CD95$^+$ NK-high' multiple sclerosis inhibit IFN-γ production by MBP-reactive T cell clones

To analyse how the NK cells from 'CD95$^+$ NK-high' multiple sclerosis efficiently control autoimmune T cell responses, we established three MBP-specific TCC from a 'CD95$^+$ NK-high' patient. These TCC proliferated and secreted IFN-γ, TNF-α, IL-2 and IL-5 in response to MBP presented by irradiated, fresh autologous PBMCs. Using the proliferation response and cytokine secretion by

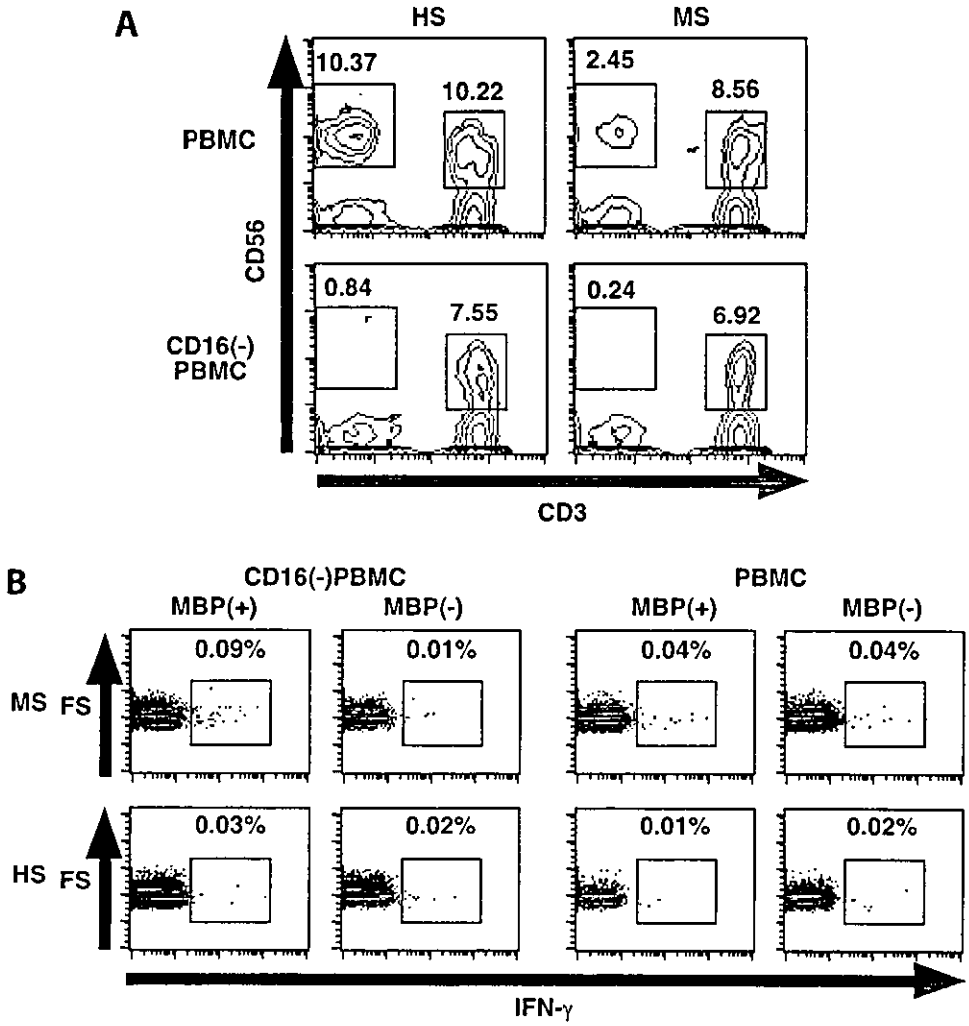

Fig. 3 Depletion of CD16$^+$ cells also allows detection of MBP-specific memory T cells in 'CD95$^+$ NK-high' multiple sclerosis. (A) Changes in the frequency of CD56$^+$ NK cells and CD56$^+$ NKT cells after deleting CD16$^+$ cells. Using CD16 microbeads, we deleted CD16$^+$ cells from PBMCs from two 'CD95$^+$ NK-high' patients and from two healthy subjects. The cells were stained with anti-human CD3-FITC and anti-CD56-PC5 to check the proportion of CD56$^+$ NK cells and CD56$^+$ T cells before and after CD16$^+$ cell depletion (upper versus lower panels). Shown are the results of a representative pair of multiple sclerosis and healthy subjects. (B) CD16$^+$-cell-depleted PBMCs from 'CD95$^+$ NK-high' multiple sclerosis responded rapidly to MBP. Using the same PBMC samples (CD16$^+$ or CD16$^-$), we conducted the IFN-γ secretion assay as described in Fig. 2A. This figure shows the result of the representative pair of multiple sclerosis patients and healthy subjects.

the TCC as read-out, we compared the whole PBMCs and the NK cell-deleted PBMCs for the ability to present whole MBP to the autologous TCC. We found that the whole PBMCs did not differ from the NK-deleted PBMCs in the ability to induce MBP-driven proliferation of TCC (Fig. 4A). However, the proportion of IFN-γ-secreting T cells among the TCC increased significantly when the NK cell-depleted PBMCs were used as antigen presenting cells (APC) (Fig. 4B). We also noticed a significant elevation of IFN-γ in the culture supernatant along with the increase of IFN-γ-secreting T cells (Fig. 4C). However, neither TNF-α nor IL-2 production was enhanced by NK cell depletion. These results support the view that NK cells from 'CD95$^+$ NK-high' multiple sclerosis regulate autoimmune T cells by inhibiting the T cell production of IFN-γ.

Discussion

It is generally held that relapse of multiple sclerosis represents the destructive CNS inflammation triggered by recently activated autoimmune T cells. In other words, pathogenic autoimmunity is apparently active during clinical relapse, which can be objectively defined by clinical status as well as MRI findings. In contrast, remission of multiple sclerosis, which is chiefly determined by exclusion of active inflammation in the CNS, may probably cover a wider range of disease states.